AD-A164 009 FEEDFORWARD CONTROL OF WAVES IN LATTICE ELEMENTS(U) 1/1
MASSACHUSETTS INST OF TECH CAMBRIDGE
J H WILLIAMS ET AL. 01 AUG 85 AFOSR-TR-85-1233
UNCLASSIFIED F49620-83-C-0092 F/G 20/11 NL

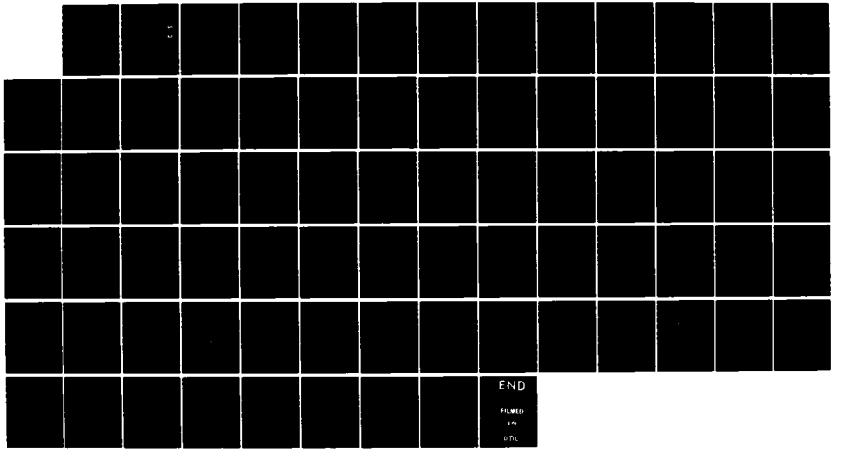

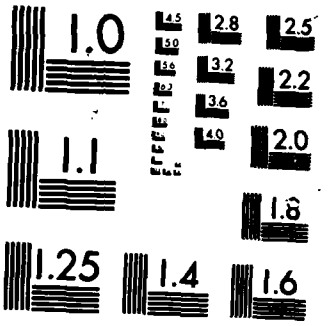

UN
SECUR

AD-A164 009

(2)

DOCUMENTATION PAGE

1a. REPORT SECURITY CLASSIFICATION: Unclassified	1b. RESTRICTIVE MARKINGS
2a. SECURITY CLASSIFICATION AUTHORITY	3. DISTRIBUTION/AVAILABILITY OF REPORT: Approved for Public Release; Distribution Unlimited.
2b. DECLASSIFICATION/DOWNGRADING SCHEDULE	
4. PERFORMING ORGANIZATION REPORT NUMBER(S)	5. MONITORING ORGANIZATION REPORT NUMBER(S): AFOSR-TR- [illegible] 1233
6a. NAME OF PERFORMING ORGANIZATION: WEA; 6b. OFFICE SYMBOL (If applicable)	7a. NAME OF MONITORING ORGANIZATION: AFOSR/NA
6c. ADDRESS (City, State and ZIP Code): P.O. Box 260, MIT Branch, Cambridge, MA 02139	7b. ADDRESS (City, State and ZIP Code): Bolling AFB DC 20332-6448
8a. NAME OF FUNDING/SPONSORING ORGANIZATION: Air Force Office of Scientific Research; 8b. OFFICE SYMBOL (If applicable): AFOSR/NA	9. PROCUREMENT INSTRUMENT IDENTIFICATION NUMBER: F49620-83-C-0092
8c. ADDRESS (City, State and ZIP Code): Bolling AFB, D.C. 20332	10. SOURCE OF FUNDING NOS.

PROGRAM ELEMENT NO.	PROJECT NO.	TASK NO.	WORK UNIT NO.
61102F	2307	B1	

11. TITLE (Include Security Classification): Feedforward Control of Waves in Lattice Elements (Unclassified)	
12. PERSONAL AUTHOR(S): James H. Williams, Jr., Gregory A. Norris and Samson S. Lee	
13a. TYPE OF REPORT: Technical	13b. TIME COVERED: FROM 1 Feb 85 TO 1 Aug 85
14. DATE OF REPORT (Yr., Mo., Day): 85 Aug 1	15. PAGE COUNT: 74
16. SUPPLEMENTARY NOTATION	

17. COSATI CODES		
FIELD	GROUP	SUB. GR.

18. SUBJECT TERMS (Continue on reverse if necessary and identify by block number): Wave Propagation; Lattice Structures; Control; Large Space Structures

19. ABSTRACT (Continue on reverse if necessary and identify by block number)

The motion in a lattice substructural element, within which longitudinal stress waves propagate nondispersively and without attenuation, is assumed to be governed by the classical wave equation. A feedforward controller configuration is proposed to isolate a portion of the substructure from longitudinal wave disturbances. The governing equations for the propagation of incoming and controller-generated stress waves in the substructure are determined.

To prevent instability, the controller must respond to incoming stress waves only, disregarding self-generated outgoing waves. The transfer function for the controlled substructure system is derived. The dependence of the transfer function magnitude on the input waveform frequency as well as on controller error parameters is demonstrated. The ranges of acceptable controller error are determined for the operational goals of disturbance cancellation and disturbance amplitude attenuation.

20. DISTRIBUTION/AVAILABILITY OF ABSTRACT: UNCLASSIFIED/UNLIMITED ☒ SAME AS RPT. ☐ DTIC USERS ☐	21. ABSTRACT SECURITY CLASSIFICATION: UNCLASSIFIED
22a. NAME OF RESPONSIBLE INDIVIDUAL: Anthony K. Amos	22b. TELEPHONE NUMBER (Include Area Code): 202/767-4935
	22c. OFFICE SYMBOL: AFOSR/NA

DTIC FILE COPY

DTIC ELECTE FEB 11 1986 D

DD FORM 1473, 83 APR — EDITION OF 1 JAN 73 IS OBSOLETE.

UNCLASSIFIED
SECURITY CLASSIFICATION OF THIS PAGE

ACKNOWLEDGMENTS

The Air Force Office of Scientific Research (Project Monitor, Dr. Anthony K. Amos) is gratefully acknowledged for its support of this research.

NOTICE

This document was prepared under the sponsorship of the Air Force. Neither the US Government nor any person acting on behalf of the US Government assumes any liability resulting from the use of the information contained in this document. This notice is intended to cover WEA as well.

TABLE OF CONTENTS

I. INTRODUCTION

Requirements for controlled structures in space for astronomy, communication networks, near-earth scientific studies, and space solar power alternatives have recently generated much interest in the active control of flexible structures [1]. Such applications typically call for very large lattice structures (up to several kilometers in extent) which would support arrays of antennae, solar cells, etc. A lattice is usually constructed by assembling many simple truss-like substructures into a large periodic structure.

The scope of the present study is limited to the active control of the propagation of vibrational disturbances in a single truss-like substructure, many of which might comprise a lattice structure. Reduction of the problem to this scale greatly simplifies the vibrational dynamics, as the effects of boundary reflections are omitted. The problem is further simplified by idealizing the substructures as thin elastic rods which are subjected only to longitudinal stress wave disturbances.

This study investigates the concept of utilizing a feedforeward controller to sense and subsequently cancel incoming longitudinal stress wave disturbances by superposing the negative of each individual disturbance. The objective of such a controller is to isolate a portion of the substructure from vibration due to incoming disturbances. While the report is primarily devoted to deriving and analyzing the response characteristics of a substructure with such a feedforeward

controller implemented, a discussion is provided in Appendix A on the response of a counterpart feedback controller. It is hoped that once developed, the ability to control the propagation of disturbances in single substructural elements may have an application to the problem of lattice-wide vibration control.

II. FORMULATION OF ROD MODEL FOR SUBSTRUCTURE

The governing equation for the propagation of longitudinal waves in thin rods is known [2]. Fig. 1 shows a straight, thin rod, where the coordinate x refers to the location of a rod cross section, and the longitudinal displacement of that cross section is given by $u(x,t)$. The rod is subjected to a stress field $\sigma(x,t)$, which may vary with position x and time t; tensile stress is assumed to be positive. The material is assumed to behave elastically, obeying the simple Hooke's law

$$\sigma = E\varepsilon \tag{1}$$

where E is Young's modulus and ε is the axial strain defined by

$$\varepsilon = \frac{\partial u}{\partial x} \tag{2}$$

In the absence of body forces, the equation of motion for the rod is given by the familiar wave equation [2]

$$\frac{\partial^2 u}{\partial x^2} = \frac{\rho}{E}\frac{\partial^2 u}{\partial t^2} \tag{3}$$

where ρ is the material mass density.

The configuration of lattice substructures is assumed to be that of thin elastic rods. It is important to note the assumptions made in deriving eqn. (3) for the thin rod model of a lattice substructure, which are as follows:

(1) The substructure is assumed to be homogeneous, so that E

and ρ do not vary with x.

(2) The substructure shape is prismatic, so that the cross sectional area A does not change with x.

(3) Uniaxial stress is assumed, and although uniaxial strain is not assumed, the inertial effects associated with lateral strain (Poisson effect) are neglected.

(4) Stresses in the substructure are assumed to be subject to no attenuation. This assumption is not unrealistic, since the vibration of many long, flexible, lightweight structures in space is very lightly damped [1].

A useful solution to eqn. (3), credited to D'Alembert (1747), is [2]

$$u(x,t) = f_1\left(\frac{x}{c_0} - t\right) + f_2\left(\frac{x}{c_0} + t\right) \tag{4}$$

where f_1 and f_2 are arbitrary functions which represent disturbances propagating at a velocity c_0; f_1 is associated with the components of the total disturbance which are travelling in the positive x direction, and f_2 represents the components travelling in the negative x direction. The velocity of longitudinal wave propagation, c_0, is determined by the material properties of the elastic solid, and is given by [2]

$$c_0 = \sqrt{\frac{E}{\rho}} \tag{5}$$

Stress wave propagation can be shown to follow the same rule of propagation. Taking the partial derivative of eqn. (3) with

respect to position gives

$$\frac{\partial}{\partial x}\left(\frac{\partial^2 u(x,t)}{\partial x^2}\right) = \frac{\partial}{\partial x}\left(\frac{\rho}{E}\frac{\partial^2 u(x,t)}{\partial t^2}\right) \tag{6}$$

which may be rewritten as

$$\frac{\partial^2}{\partial x^2}\left(\frac{\partial u(x,t)}{\partial x}\right) = \frac{\partial^2}{\partial t^2}\left(\frac{\rho}{E}\frac{\partial u(x,t)}{\partial x}\right) \tag{7}$$

Next, eqn. (2) is used to write

$$\frac{\partial^2 \varepsilon(x,t)}{\partial x^2} = \frac{\rho}{E}\frac{\partial^2 \varepsilon(x,t)}{\partial t^2} \tag{8}$$

which, from Hooke's Law and the homogeneity criterion, becomes

$$\frac{\partial^2 \sigma(x,t)}{\partial x^2} = \frac{\rho}{E}\frac{\partial^2 \sigma(x,t)}{\partial t^2} \tag{9}$$

The D'Alembert solution form thus pertains for stress wave propagation as well, so that it is possible to write

$$\sigma(x,t) = g_1\left(\frac{x}{c_0} - t\right) + g_2\left(\frac{x}{c_0} + t\right) \tag{10}$$

where g_1 and g_2 are arbitrary functions that will be specifically determined by the initial conditions or forcing function in a given problem.

Eqn. (10) describes stress waves which propagate without distortion or attenuation through the substructure. Thus, input waves of arbitrary "shape" propagating in the positive x direction past point x_1 in the rod of Fig. 1 will later pass point x_2 unchanged from their original configuration.

This nondispersive characteristic may be expressed as

$$\sigma^+(x_2,t) = \sigma^+(x_1, t-\tau_{12}) \tag{11}$$

where $\sigma^+(x_2,t)$ denotes the magnitude of a stress wave at cross section x_2 at time t, as the wave propagates through the substructure. The superscript "+" indicates that propagation is in the positive x direction, and τ_{12} is the time constant associated with the "transportation lag" [3] of propagation along a length ℓ_{12} of the substructure between sections x_1 and x_2 .

$$\tau_{12} = \frac{x_2 - x_1}{c_0} = \frac{\ell_{12}}{c_0} \tag{12}$$

Nondispersive, unattenuated propagation is illustrated in Fig. 2, which shows a schematic of a stress wave propagating through the substructure of Fig. 1. In Fig. 2a a rightwardly-propagating stress wave of arbitrary shape is shown with its wavefront located at cross section x_1 at time t_0. Then, after a time duration of τ_{12} has elapsed, the wave has propagated to the right so that its wavefront is located at cross section x_2 as shown in Fig. 2b; the shape of the wave is unchanged. After an elapsed time of τ_{13}, which is given by

$$\tau_{13} = \frac{x_3 - x_1}{c_0} = \frac{\ell_{13}}{c_0} \tag{13}$$

the wavefront has reached cross section x_3 as shown in Fig. 2c, with the wave shape undistorted and the amplitude unchanged.

The delay function related by eqn. (11) may be given a block diagram representation, as in Fig. 3, where the nodes x_1 and x_2

refer to the corresponding substructure cross sections, and double-lined faces on the delay block are used to distinguish it from typical constant-multiplier blocks. Block diagram representations will be useful later in visualizing the overall structure of the control system under study.

The operation represented by the delay block shown in Fig. 3 is simple; its output signal or function is merely the input signal or function delayed by the time constant with which the particular block is labelled. Thus in Fig. 3 the output stress function $\sigma^+(x_2,t)$ is merely the delay of the input stress function $\sigma^+(x_1,t)$. Since the time delay for wave propagation between x_1 and x_2 is given by eqn. (12) as τ_{12}, then eqn. (11) describes the operation of the delay block in Fig. 3. Note also that eqns. (12) and (13) may be generalized in the following form:

$$\tau_{mn} = \frac{|x_n - x_m|}{c_0} = \frac{\ell_{mn}}{c_0} \tag{14}$$

where τ_{mn} is the time delay for longitudinal wave propagation in either direction between two cross sections x_m and x_n.

Before addressing the control problem, two other aspects of wave propagation in the lattice substructure will be discussed and represented by block diagram elements, which will subsequently be used to illustrate the different configurations and the underlying assumptions of a few different controller designs.

First, waves may propagate through the substructure in either the positive or negative x-directions, as shown in eqn.

(10). Thus, in Fig.4, $\sigma^{+}(x_1,t)$ is shown passing through the delay block in the positive x direction (from x_1 to x_2), and $\sigma^{-}(x_2,t)$ is shown passing through the same delay block in the negative x direction (from x_2 to x_1).

The second aspect is the principle of superposition in linear systems. When two waves travelling in a lattice substructure pass the same location, their magnitudes at that cross section are additive. This superposition principle is accounted for by summing the values of time functions for leftwardly and rightwardly propagating stress functions at a cross section in order to obtain the net time function for stress at that cross section. Fig. 4 shows the standard block diagram notation for such a summation operation. Just as the net or actual value of stress at a physical cross section is the sum of the instantaneous values of propagating stress waves at that cross section, likewise the stress value at a given cross section in the block diagram is the sum of both the leftwardly and rightwardly propagating stress functions for the cross section at that point in time.

To illustrate the superposition principle, successive stress pulse diagrams are shown in Fig. 5, for the special case where τ_{12} is equal to τ_{23} (that is, the distance ℓ_{12} between sections x_1 and x_2 is equal to the distance ℓ_{23} between sections x_2 and x_3.)

In Fig. 5, two waves are shown approaching cross section x_2 from opposite directions. The speed of propagation for all longitudinal stress waves in the substructure is given by eqn.

(5). Fig. 5 shows both waves propagating at equal speed until they are fully superposed at time t equal to $t_0 + \tau_{12}$. During superposition the waves partially cancel; their separate magnitudes are represented by outlines, and their sum or net magnitude is shaded. After superposition the waves continue to propagate in their respective directions undistorted, as Fig. 5 shows. Fig. 6 shows a block diagram model for this length of the substructure from section x_1 to x_3.

III. FORMULATION OF FEEDFOREWARD CONTROL MODEL

A. Idealized Controller Components

The principle of waveform superposition underlies the scheme to be analyzed for vibration control in this study--namely, cancellation of propagating stress waves by generating and superposing the negative of waveform disturbances contained in the structure. The analysis will consider disturbance (input) waves which are propagating through a lattice substructure in the positive x direction, as well as the operations of a controller designed to protect the region of the substructure to the right of section x_2 (refer to Fig. 1).

The operations of the ideal feedforeward controller to be studied may be described as follows. First, a sensor at section x_1 is used to measure the amplitude of the stress wave disturbance as it passes the section. The signal generated by the sensor is delayed, and provides input to the actuator at cross section x_2, where the negative of the incoming stress wave is actuated after an appropriate time delay. As indicated in eqn. (12), the length of the time delay will be determined by the distance ℓ_{12} along the substructure between the sensor and the actuator.

It is important to clearly state the assumptions which are involved in the simplified modelling of the sensor, delayer, and actuator elements in this idealized controller design. They are as follows:

(1) Sensor-- The sensor is assumed to be a transducer of negligible size and mass which is fixed to the substructure at section x_1, and which generates a signal s(t) (with units of volts) proportional to the longitudinal stress at the section, $\sigma(x_1,t)$.

$$s(t) = \frac{1}{G_1}\sigma(x_1,t) \tag{15}$$

Here $(1/G_1)$ is the constant of proportionality (or "gain") associated with the sensor, and has units of (volt/psi). The actual operating principle (piezoelectric, electromechanical, strain-resistive, etc.) is not considered in the present analysis.

(2) Delayer-- The signal s(t) is fed to a signal delay element, whose output s'(t) is given by

$$s'(t) = s(t-\tau'_{12}) \quad ; \text{ for } t \geq \tau'_{12} \tag{16}$$

where τ'_{12} is the time delay introduced by the delayer. In the case of ideal operation, τ'_{12} will equal τ_{12}, which is the actual transportation lag of stress waves propagating from section x_1 to section x_2.

(3) Actuator-- The actuator is located at a particular section in the rod, x_2. It is approximated by a disk whose thickness is negligible and whose impedance is matched to that of the rod, so that stress waves propagate past cross section x_2 unaffected by the presence of the actuator.

It is assumed that the controller can apply a time varying axial force F(t) to the disk, and that the value of F(t) is

proportional to the signal s'(t) received from the delayer.

$$F(t) = G_2 \cdot s'(t) \tag{17}$$

Here, G_2 is the actuator gain, and has units of (lb/volt).

Once again, the present analysis does not consider whether the force is actually generated piezoelectrically, electromagnetically, etc. What is important is that the controller is assumed to generate time-varying uniform stress distributions across the faces of the substructure.

b. Description of Actuator Operation

Fig. 7a shows the idealized actuator-substructure assembly intact, where the rod has cross sectional area A. In Fig. 7b segments of the lattice substructure have been isolated as free body diagrams, to show the applied forces and resultant stresses. In Figs. 7a and 7b, the positive x direction is indicated and tensile stresses are defined positively as shown.

It is necessary to derive expressions for the applied stress functions $\sigma_1(t)$ and $\sigma_2(t)$ in the substructural element. Examining Fig. 7b, a balance of forces can be written for the massless actuator component.

$$\Sigma F_x = 0 = F(t) + A \cdot \sigma_2(t) - A \cdot \sigma_1(t) \tag{18}$$

$$\text{Therefore,} \quad F(t) = A[\sigma_1(t) - \sigma_2(t)] \tag{19}$$

Geometric compatibility requires that displacements and velocities at the actuator interface be equal. Thus,

$$u_1(t) = u_2(t) \tag{20}$$

$$\frac{\partial u_1(t)}{\partial t} = \frac{\partial u_2(t)}{\partial t} \tag{21}$$

Next, the cross sectional velocities can be expressed in terms of the stresses on the corresponding faces [2].

$$\frac{\partial u_1(t)}{\partial t} = \frac{c_0}{E}\sigma_1(t) \tag{22}$$

$$\frac{\partial u_2(t)}{\partial t} = \frac{c_0}{E}\sigma_2(t) \tag{23}$$

Combining eqns. (20) through (23) yields the requirement on the stresses as

$$\frac{c_0}{E}\sigma_1(t) = \frac{-c_0}{E}\sigma_2(t) \tag{24}$$

Therefore,

$$\sigma_1(t) = -\sigma_2(t) \tag{25}$$

This result, together with the force balance relation, (eqn. (19)), gives the expressions for the resultant stress functions at the actuator in terms of the forcing function as

$$\sigma_1(t) = \frac{F(t)}{2A} \tag{26}$$

$$\sigma_2(t) = \frac{-F(t)}{2A} \tag{27}$$

Finally, it is necessary to write expressions for the propagation characteristics of the stress waves which the

actuator, as described above, serves to generate at the actuator-substructure faces. Conceptual division of the substructure as shown in Fig. 7 indicates the approach: the problem may be divided into two cases of longitudinal end-actuation of semi-infinite thin rods, with a stress discontinuity at cross section x_2 .

From the end-actuation analogy, the stress waves generated on the substructure face to the right of the actuator, $\sigma_2(t)$, must propagate into this "semi-infinite half" of the substructure; that is, they must propagate in the positive x direction. Thus, the equation for the propagation of controller-induced stress waves in the portion of the rod to the right of the actuator can be written by selecting the appropriate term from the D'Alembert solution to the wave equation.

$$\sigma^{+}(x,t) = \frac{-1}{2A} \cdot F\left(\frac{x-x_2}{c_0} - t\right) \quad ; \quad \text{for} \quad x > x_2 \ , \quad t \geq 0 \qquad (28)$$

The superscript "+" denotes the propagation of these stress waves in the positive x direction. Note that the argument of the function F in eqn. (28) is in units of time, not position; the function continues to represent a wave travelling in the x direction at a speed c_0 .

Likewise, actuated stress waves which are generated on the substructure face to the left of the actuator must travel to the left, again based on the division of the problem into two cases of end-actuation of semi-infinite substructures. Thus, the equation for these leftwardly-propagating stress waves also takes the form of the appropriate term from the D'Alembert solution as

$$\sigma^{-}(x,t) = \frac{1}{2A} \cdot F\left(\frac{x-x_2}{c_0} + t\right) \quad ; \quad \text{for} \quad x < x_2 \ , \ t \geq 0 \qquad (29)$$

Together, eqns. (28) and (29) summarize the results for propagating stress waves which are generated by the actuator, and they express the waves in terms of the value of the actuator forcing function, $F(t)$. Using eqns. (15) to (17), eqns. (28) and (29) for the controller-induced stress waves may be expressed as functions of the stress detected by the sensor at section x_1 .

$$\sigma^{+}(x,t) = \frac{-G_2}{2AG_1} \cdot \sigma\left[x_1, \left(\frac{x-x_2}{c_0} - t + \tau'_{12}\right)\right] \quad ; \qquad (30)$$

$$\text{for} \quad x > x_2 \ , \ t \geq \tau'_{12}$$

$$\sigma^{-}(x,t) = \frac{G_2}{2AG_1} \cdot \sigma\left[x_1, \left(\frac{x-x_2}{c_0} + t - \tau'_{12}\right)\right] \quad ; \qquad (31)$$

$$\text{for} \quad x < x_2 \ , \ t \geq \tau'_{12}$$

Fig. 8 presents a schematic of the actuator output response to the arbitrary actuator input signal $s'(t)$ shown. Fig. 9 shows a modified block diagram, composed of the elements discussed in Section II, which models the general response of the controlled substructure to a stress wave disturbance originating at x_0, with the controller formulated as above. In Fig. 9, solid arrows continue to represent the "flow" or travel of stress wave functions, while dashed lines have been used to represent (electrical) signal flow in the controller.

IV. RESPONSE OF THE CONTROLLED SUBSTRUCTURE

It is now possible to analyze the response of the controlled lattice substructure to an arbitrary input disturbance at x_0. Two important features characterize the response of the system as it is presently formulated.

The first may be likened to the "stress intensification" phenomenon which is characteristic of stress wave reflection from a fixed boundary (such as a rigid wall). As part of a wave reflects back from a fixed boundary, it may be superimposed with the still-incoming portion of the wave, so that higher amplitude transient waveforms result. The same effect is the result of the superposition of incoming waves approaching the actuator at x_1 from x_0 and the already-actuated, leftwardly-propagating stress waves, which are duplicates of previously incoming waves.

The series of pulse diagrams for $\sigma(x, t)$ in Fig. 10 illustrate this phenomenon. In Fig 10, stress pulses with dashed outlines represent stress waves generated by the controller actuator. Pulses with solid outlines are those of incoming stress wave disturbances. Consistent with all stress pulses presented in this study, the shaded portion of a pulse represents the net, or physically realized magnitude of the stress waves in the substructure.

Thus, in Figs. 10c through 10f, the incoming stress wave (solid outline) is completely cancelled by the rightwardly propagating controller-generated stress wave (dashed outline, for $x > x_2$), so that both are left unshaded, indicating that their net magnitude is zero. They superpose and cancel, so that the

portion of the lattice substructure to the right of the controller is isolated from any stress disturbance by the incoming wave. Note that in Fig. 10 τ_{12}' is assumed to be equal to τ_{12}.

In Fig. 10c the phenomenon of stress intensification is shown. The leftwardly-propagating stress wave generated by the controller is momentarily superposed on a portion of the incoming wave disturbance which is travelling to the right past section x_2 ; the result of this superposition is transient stress values which are of higher magnitude than either of the two waves' peak values alone.

There is a second problematic feature of the controller. Note that in Fig. 10e, the leftwardly-propagating stress wave (which is generated by the actuator as it also produces the negative of the incoming wave), is passing the sensor located at cross section x_1 . As the controller is presently formulated, both incoming (rightwardly-propagating) stress waves and outgoing (leftwardly-propagating) stress waves are sensed by the controller as "substructure disturbances". That is, the sensor currently generates a signal (delayed for input to the actuator) based on the instantaneous magnitude of any stress wave passing the cross section x_1 , regardless of the wave's source.

For example, the stress waves shown in Fig. 10g are being generated by the actuator as a result of the outgoing stress wave which is shown passing the sensor earlier in Fig. 10e. Note that the leftward-propagating wave generated in Fig. 10g will in turn pass the sensor. Thus, a single, non-repeated incoming stress

pulse, though cancelled perfectly by the controller, will nonetheless initiate a process of endless controller "echoing", as leftwardly-propagating controller-generated stress waves are repeatedly sensed, producing new actuations.

These two problematic features of the controller, namely stress intensification (Fig. 10c) and "echoing", (Figs. 9g and 9n) can be compounded to the degree that the system becomes unstable in response to disturbances.

Fig. 11 shows how such instability can arise in response to a simple step stress disturbance. Dashed lines again represent the outlines of controller-generated stress waves. The dashed outline of these actuated waves is shown slightly below the solid outline of the incoming stress wave for clarity only; such a representation is intended to indicate equal magnitude nonetheless. As in Fig. 10, Fig. 11 assumes that $\tau_{12}' = \tau_{12}$.

Fig 11b shows that "stress intensification", or additive superposition, has begun to occur by t equal to $t + \tau_{12}/2$, so that a wave of twice the amplitude of the incoming wave results. As the outgoing actuated wave propagates further to the left, so does the additive effect of its superposition with the incoming wave. By Fig. 11d, when t equals $t_0 + (3/2)\tau_{12}$, the higher amplitude wave has passed the sensor at cross section x_1. Accordingly, as shown in Fig. 11f, the actuator begins to generate a stress wave of twice the incoming wave's amplitude at a time which is $3\tau_{12}$ after the incoming wavefront initially passed the sensor.

Figs. 11f and 11g show that as the generated waves continue to superpose with the incoming wave, then cancellation is no

longer achieved to the right of x_2, because the controller generates waves which are twice the necessary amplitude. Finally, Fig. 11g further shows that higher amplitude waves will continue to pass the sensor, leading to generated waves of still greater amplitude. The system is unstable in response to a step input.

Fig. 12 illustrates the case for a step sinusoidal input. Again, the leftwardly-propagating waves which are generated by the controller (as it operates to cancel the incoming waves) superpose with the incoming stress waves. Stresses of double the peak amplitude of the incoming wave are subsequently measured by the sensor at x_1 (see Fig. 12e), and the controller is required to generate waves of increasingly higher amplitude (dashed outlines in Figs. 12g and 12h). Thus the system is potentially unstable in response to a step sinusoidal input.

V. CONTROLLER STABLIZATION

A preliminary approach for actively controlling the propagation of longitudinal vibrations in an idealized lattice substructure has been discussed in Sections II through IV. As developed in Section IV, the controlled substructure system is unstable in response to input disturbances. The instability arises because the sensor responds to both incoming and controller-generated leftwardly-propagating stress waves indiscriminately. It is desirable to modify the controller to prevent this instability.

One solution is to redefine the operational characteristics of the sensor. It is reasonable to assume a sensor which is sensitive only to waves propagating in the desired direction--in this case, the positive x direction. Employing such a sensor, the controller would not be reactivated by the leftwardly-propagating stress waves which the actuator generates, and thus the system would not exhibit the instability characteristics discussed in Section IV.

A second, more general solution to the problem of instability would be to add a loop to the controller which effectively deducts the delay of the actuator output from the sensor's output. Implementation of this solution is illustrated by a block diagram representation in Fig. 13. As shown in Fig. 13, the signal which provides input to the actuator is also fed back to be subtracted from the sensor output, through a delayer labeled τ_{12}''. Since the objective of this additional loop is to deduct from s(t) that portion of the signal which corresponds

to the leftwardly-propagating (actuator-generated) portion of $\sigma(x_1,t)$, then it is necessary that τ_{12}'' be exactly equal to τ_{12} in order to totally cancel the actuator-generated portion of $\sigma(x_1,t)$. A nonzero difference between τ_{12}'' and τ_{12} is thus an additional possible source of controller error; the effects of such a nonzero difference will not be analyzed here, but the study of such effects constitutes an appropriate topic for further research.

For the remaining analysis, the successful application of this latter more general stabilized method to the controller will be assumed. Thus, in the remaining analysis, it is assumed that τ_{12}'' equals τ_{12}, so that the deduction of the delayed value of s'(t) from the sensor output occurs at precisely the same instant that the sensor is measuring the leftwardly-propagating disturbance which was generated in response to s'(t) and which has travelled back through the substructure from x_2 to x_1. The response of the controlled lattice substructure to a step input disturbance, following this controller modification, is shown in Fig. 14. In Fig. 14, the effect of stress intensification has propagated back past the sensor at section x_1 by time t equal to $t_0 + 2\tau_{12}$. However, as Fig. 14 shows, for time t equals $3\tau_{12}$ and beyond, the actuator never doubles the value of the controller-generated wave, because a value associated with the leftwardly-propagating disturbance is effectively subtracted from the sensor output, as schematized in Fig. 13. Fig. 14 may be compared with Fig. 11, discussed in Section IV, which illustrates the response of the unmodified controller-substructure assembly to an identical step input disturbance.

VI. INPUT/OUTPUT CHARACTERISTICS OF STABLIZED FEEDFOREWARD-CONTROLLED SUBSTRUCTURE

A. Transfer Function Magnitude

It is useful to characterize a linear system by its transfer function, or (steady state) frequency response, $H(\omega)$, which is given by

$$H(\omega) = \frac{Y(\omega)}{X(\omega)} \tag{32}$$

where ω denotes radian frequency, $X(\omega)$ is a steady harmonic input to the system and $Y(\omega)$ is the system output. The transfer function for the feedforeward-controlled substructure which has been treated in the previous sections is derived in Appendix E, and found to be given by

$$H_f(\omega) = e^{-i\omega\tau_{12}} - Ke^{-i\omega\tau_{12}'} \tag{33}$$

where τ_{12} and τ_{12}' are the time delays for wave propagation through the substructure and the controller, respectively; the controller net feedforeward amplification, given by $G_2/2AG_1$ in Section III, has been replaced by K for simplicity; and $i = \sqrt{-1}$.

It can be seen from eqn. (33) that the transfer function is a complex function. Defining

$$\varepsilon = \tau_{12}' - \tau_{12} \tag{34}$$

where ε denotes the difference between the time delay of waves propagating in the substructure τ_{12} and the delay of the controller τ_{12}', then Appendix B shows that the square of the transfer function magnitude is given by

$$|H_f(\omega)|^2 = 1 - 2K\cos(\omega\varepsilon) + K^2 \qquad (35)$$

In terms of the controlled substructure system under study, the magnitude of the transfer function given in eqn. (35) represents the complex magnitude of the ratio of the system output to the system input where both are expressed as complex functions in the frequency domain. In the time domain, the system input and output are assumed to be stress functions $\sigma^+(x_1, t)$ and $\sigma(x_3, t)$, respectively, both are representable by harmonic components, x_1 and x_3 denote the locations of cross sections on the substructure as shown in Fig. 9, and the superscript "+" indicates that only stress waves propagating in the positive x direction past section x_1 are actually input into the system.

As long as the time domain input and output of the controlled substructure are sinusoidal stress functions with frequency ω, a transfer function magnitude $|H_f(\omega)|$ of less than unity represents system attenuation of an input stress function. A transfer function magnitude equal to zero represents complete attenuation or cancellation of the input stress function. A transfer function magnitude $|H_f(\omega)|$ greater than unity indicates controller operation which effectively amplifies incoming sinusoidal stress functions of frequency ω, so that the amplitude of the stress wave output to cross section x_3 in Fig. 9 is greater than that of the input stress wave.

b. Operational Ranges of Controller Error

Two types of controller error are considered in this study: (1) nonzero values for the difference between controller and substructure delays, ε, which is given by eqn. (34); and (2) values of the net feedforeward controller gain K not equal to the substructure gain of unity.

There are also two possible operational goals for the feedforeward controller, within the broad domain of "active vibration control". The first possible goal is "ideal" controller performance--achieving complete superpositional cancellation of the incoming stress wave disturbance, thus completely isolating cross section x_3 from any (rightwardly-propagating) vibrational disturbances (see Fig. 9). The second, more modest goal of controller implementation would be achievement of disturbance attenuation, if not full cancellation. In this case the objective might be an output stress wave whose amplitude is some fraction of the input disturbance amplitude, thus requiring a transfer function magnitude less than unity. The present subsection identifies the allowable ranges of controller error for achievement of each of these two controller objectives.

(1) Achieving complete disturbance cancellation

"Ideal" operation of the controller calls for complete cancellation of incoming stress wave disturbances which are input to the controlled substructure system. It is possible to derive

the requirements on the controller delay error, ϵ , given by eqn. (34), and the requirements on the net feedforward controller gain K.

Eqn. (35) gives the expression for the square of the system transfer function magnitude. Achievement of full input disturbance cancellation requires a system output of zero, and thus a transfer function magnitude of zero. With this requirement on $|H_f(\omega)|$, eqn. (35) becomes

$$K^2 - 2K\cos(\omega\epsilon) + 1 = 0 \tag{36}$$

Eqn. (36) is a quadratic equation, so that its solution is given by

$$K = \frac{2\cos(\omega\epsilon) \pm \sqrt{\left[-2\cos(\omega\epsilon)\right]^2 - 4}}{2} \tag{37}$$

which may be simplified and rewritten as

$$K = \cos(\omega\epsilon) \pm \sqrt{\cos^2(\omega\epsilon) - 1} \tag{38}$$

Eqn. (38) is the requirement for full controller cancellation of incoming disturbances. If K, the controller feedforward gain, is to take on only real values, then the difference under the radical in eqn. (38) must be nonnegative. This requirement states that

$$\cos^2(\omega\epsilon) \geq 1 \tag{39}$$

and thus ideal controller operation requires that

$$\omega\varepsilon = \pi n \tag{40}$$

where n is any integer, n = ...-2,-1,0,1,2....

Using the relation

$$T = \frac{2\pi}{\omega} \tag{41}$$

where T is the period (in seconds) of a sinusoidal waveform with radian frequency ω, the requirement on the controller delay error (eqn. (40)) can be rewritten

$$\varepsilon = \frac{1}{2}(nT) \tag{42}$$

Eqn. (42) indicates that for complete cancellation of a sinusoidal input disturbance, the duration of the controller delay error ε must be equal to some integer multiple of half the input waveform period T.

Next, combining eqns. (40) and (38) yields

$$K = \begin{cases} 1 & \text{for n even} \\ -1 & \text{for n odd} \end{cases} \tag{43}$$

which is the second requirement on the controller parameters which must be fulfilled if the controller is to operate ideally.

Thus, in summary, for the controller to operate such that complete cancellation of input disturbances is achieved, both eqns. (42) and (43) must be satisfied simultaneously by the controller parameters.

(2) Achieving disturbance attenuation

In the case where the goal of controller implementation is achieving attenuation of stress wave disturbances which are input to the system, it is necessary that for an input sinusoidal stress function of radian frequency ω, the magnitude $|H_f(\omega)|$ of the system transfer function must be less than unity. Solving eqn. (35) for this requirement yields

$$1 > 1 - 2K\cos(\omega\varepsilon) + K^2 \tag{44}$$

Eqn. (44) may be simplified to obtain

$$\begin{aligned} K &< 2\cos(\omega\varepsilon) \quad ; \quad \text{for } K > 0 \\ K &> 2\cos(\omega\varepsilon) \quad ; \quad \text{for } K < 0 \end{aligned} \tag{45}$$

Eqn. (45) is plotted in Fig. 15, where all value pairs for K and $\omega\varepsilon$ which satisfy the inequality lie in the shaded portion of tne plane, but do not include the points where the line $K=2\cos(\omega\varepsilon)$ crosses the $(\omega\varepsilon)$axis.

Examination of Fig. 15 and eqn. (45) indicates that while there are no upper or lower bounds for acceptable values of the parameter $(\omega\varepsilon)$, the magnitude of the controller feedforward gain K must never reach or exceed a value of 2 if attenuation is to be achieved. Also, the parameter $(\omega\varepsilon)$ must not equal any odd integer multiple of $\pi/2$, and the parameters K and $(\omega\varepsilon)$ cannot be set independently, if attenuaticn is to be achieved.

C. Physical Basis for Frequency Dependence of Transfer Function Magnitude

Eqn. (35), the expression for the magnitude of the controlled substucture system transfer function, is plotted in Fig. B-3 as the transfer function magnitude squared, $|H_f(\omega)|^2$, versus the parameter $\omega\varepsilon$. Eqn. (35) and Fig. B-3 show that the magnitude of the transfer function depends on the frequency ω of the incoming disturbance. That is, for a constant feedforward gain K and a constant difference ε between substructure and controller delays, the magnitude of the system transfer function will be different for different input signal frequencies. Therefore, since actual inputs to the controlled-substructure system may be waveforms composed of several harmonics at different frequencies, the magnitude of certain such harmonics will be enhanced in the system response while that of harmonics at other frequencies will be diminished. In fact, as Fig. B-3 illustrates, the magnitude of the transfer function is periodic in $\omega\varepsilon$. That is, as $\omega\varepsilon$ is increased (or decreased) by 2π, the magnitude of the transfer function repeats itself.

To understand physically the dependence of the system transfer function magnitude on the input waveform's harmonic frequencies, it is useful to introduce the concept of a waveform period. Making use of eqn. (41), where T is the period (in seconds) of a waveform whose radian frequency is ω, note that

$$\omega\varepsilon = 2\pi\left(\frac{\varepsilon}{T}\right) \tag{46}$$

Substituting eqn. (46) into eqn. (35) then gives

$$|H_f(2\pi/T)|^2 = 1 - 2K\cos\left[2\pi\left(\frac{\varepsilon}{T}\right)\right] + K^2 \qquad (47)$$

Eqn. (47) is plotted in Fig. 16 to illustrate that the magnitude of the transfer function is periodic in (ε/T). It is instructive to consider that the ratio (ε/T) is a measure of ε as a percentage of the waveform period. For a waveform with constant period T, Fig. 16 shows that as the difference in the controller and substructure time delays ε is increased from 0 to 50 percent of T, the magnitude of the transfer function is increased from its minimum to its maximum value.

As developed in Section VI-B, only when the magnitude of the net controller gain equals unity is it possible for the controlled system to completely attenuate incoming signals. Figs. 16 and B-3 present the frequency dependency of the transfer function magnitude for the general case where K is unspecified. The remaining analysis will assume K equal to unity, (zero gain error), and will quantify the effects of controller delay error given this assumption.

Fig. 17 is a plot of the square of the system transfer function magnitude versus the parameter (ε/T), with K set equal to unity. Of particular interest is the dashed horizontal line in Fig. 17 representing a transfer function magnitude of unity. Above this line the controlled system amplifies an input disturbance; below it the input is attenuated.

Eqn. (45) may be solved for K equal to unity to determine the ranges of the parameter (ε/T) over which the system

attenuates an input. Eqn. (45) becomes

$$\cos(\omega\varepsilon) > 1/2 \tag{48}$$

which can be rewritten, using eqn.(41), as

$$\cos\left[2\pi\left(\frac{\varepsilon}{T}\right)\right] > 1/2 \tag{49}$$

Eqn. (49) is solved for (ε/T) in the following ranges:

$$(n - 1/6) < \frac{\varepsilon}{T} < (n + 1/6) \tag{50}$$

where n is any integer.

Eqn. (50) thus specifies the ranges of the parameter (ε/T) for which the feedforward controlled substructure system successfully attenuates an incoming stress wave disturbance for K equal to unity.

When the feedforward gain is held constant at unity, then for (ε/T) in the ranges (n-1/6 to n+1/6) where n is any integer, the system attenuates a steady sinusoidal input signal. Likewise, for (ε/T) in the ranges (n+1/6 to n+5/6) the system amplifies a steady sinusoidal input signal.

Mathmatically, this result is found by solving eqn. (48) when K and $|H_f(2\pi/T)|$ are both equal to unity. Physically, it arises because for (ε/T) in the ranges (n-1/6 to n+1/6) the sinusoidal output of the controller and substructure tend to subtract in phase, while for (ε/T) in the ranges (n+1/6 to n+5/6) the controller and substructure output tend to add in phase.

Fig. 18 presents graphically the relationship discussed

above for ε as a varying percentage of a constant period T, and K equal to unity. Fig. 18 shows the stress at location x_2 as a function of time for a sinusoidal input of unit amplitude. In Fig. 18a $\varepsilon = 0$, so that the substructure output stress function at cross section x_2 (solid line) and the controller output stress function at cross section x_2 (dashed line) subtract completely (that is, they are exactly 180 degrees out of phase); and the magnitude of their sum is equal to zero everywhere. This is the case of ideal controller operation (feedforward gain K equal to unity and the controller delay exactly equal to the substructure delay), in which complete superpositional cancellation is achieved.

In Fig. 18b (ε/T) equals 1/6, and the system output waveform (the sum of the controller and substructure outputs) is indicated by the shading. Fig. 18b shows that the peak amplitude of the system output is equal to the peak amplitude of the substructure output (and thus that of the input signal, since the substructure gain is equal to unity), which indicates that the magnitude of the transfer function is unity for K equal to unity and for (ε/T) equal to 1/6.

In Fig. 18c, (ε/T) equals 1/2. Substructure and controller output add in phase in Fig. 18c, yielding an output waveform whose peak amplitude is twice that of the substructure output, and thus is also twice that of the input waveform. In this case then, the magnitude of the transfer function is equal to 2, which is identical to the result shown for K equal to unity and (ε/T) equal to 1/2 in Fig. 17 and eqn. (47).

Finally, Fig. 18d shows the system response when (ε/T) equals unity. The results are indistinguishable from those in Fig. 18a, illustrating the periodicity of $|H_f(2\pi/T)|$ with respect to (ε/T). When the controller output waveform leads or lags the substructure output waveform by ε equal to any integer multiple of the period (in this case the integer is unity) then the two output waveforms are superposed exactly 180 degrees out of phase, and thus they completely cancel.

In actual operation of the controlled substructure system, it is more likely that the delay error ε, given by eqn. (34), will be fixed and the system will be subject to an input composed of numerous harmonics which are distributed over a range of frequencies. The magnitude of the transfer function for each harmonic will vary according to the particular harmonic's frequency in a manner dictated by eqn. (47) and identical to that discussed above and presented in Fig. 18. The parameter $1/T$ varies linearly with the radial frequency ω, as eqn. (41) indicates, so that for higher frequencies the period T is shortened and a constant ε becomes a larger percentage of T, increasing the ratio (ε/T). The consequent frequency dependence of the transfer function magnitude is presented graphically in Fig. 19, for which ε is constant, K is held equal to unity, and the input waveform's frequency (and thus its period) are varied.

When a waveform's period is equal to 6ε, then (ε/T) equals 1/6, and $|H_f(2\pi/T)|$ is equal to unity (for K equal to unity). This case is shown in Fig. 19a, where the substructure and controller outputs are represented by solid and dashed lines,

respectively, and their sum (the system output) is shaded.

In Fig. 19b, the frequency has increased to 3 times its value in Fig. 19a, reducing the period to twice the length of ε, so that the controller and substructure outputs are exactly in phase. In this case the controller and substructure outputs additively superpose to produce a system output whose magnitude is twice the magnitude of the input (that is, twice the magnitude of the unity-gain substructure's output). This transfer function magnitude of $|H_f(2\pi/T)|$ equal to 2 is exactly the magnitude specified in Fig. 17 for (ε/T) equal to 1/2 and K equal to unity.

Finally, in Fig. 19c, the frequency is 6 times its value in Fig. 19a, so that T now equals ε exactly, and the controller and substructure outputs are exactly half a period out of phase so that they cancel entirely. This case illustrates complete input attenuation, ($|H_f(2\pi/T)|$ equals 0), which is what eqn. (47) and Fig. 17 give when K equals unity and (ε/T) takes on an integer value.

Together, Figs. 18 and 19 provide several system output examples which illustrate the physical basis for the frequency dependence of the controlled substructure transfer function magnitude. This dependency is derived in Appendix B, and is presented in eqns. (35) and (47), and in Figs. B-3 and 16.

VII. CONCLUSIONS AND RECOMMENDATIONS

To avoid instability, a feedforward controller used to actively control wave propagation in lattice substructures should be designed to effectively sense and cancel only incoming disturbances. This may be achieved by utilizing a unidirectional sensor; a more generally applicable solution is to add a correction feedback loop in the controller.

Two possibilities for controller error include: (1) a net feedforward controller gain that does not match that of the substructure; and (2) a controller delay time which differs from the time required for wave propagation through the substructure.

If full cancellation of incoming sinusoidal disturbances is to be achieved for the portion of the substructure beyond the controller, the controller feedforeward gain amplitude must match that of the substructure exactly. If attenuation is to be achieved, the controller gain amplitude must be less than twice that of the substructure.

For a nonzero discrepancy between the controller delay and the delay for wave propagation in the structure, the ratio of the system (sinusoidal) output amplitude to the input sinusoidal amplitude is dependent on the input waveform's radian frequency.

To fully cancel sinsuoidal disturbances in the substructure beyond the controller, assuming matched controller and substructure gains, the duration of the controller-substructure delay discrepancy must be equal to an integer multiple of half the input waveform period. To attenuate incoming disturbances, assuming matched controller and substructure gains, the delay

discrepancy must not differ from an integer multiple of the input waveform period by more than one sixth of the period duration. This range approaches zero as the magnitude of K approaches 2, and becomes larger as the magnitude of K approaches zero.

Further work should be done to determine analytically the dependence on frequency and on controller error of the ratio of output to input wave energies. The effects of delay error in the stabilizing feedback loop should be analyzed.

The analytical results contained here should also be verified experimentally.

REFERENCES

[1] R.E. Skelton, "On the Control Design of Flexible Spacecraft", Theory and Application of Optimal Control in Aerospace Systems, AGARDograph No. 251, NATO, Neuilly Sur Seine, France, 1982.

[2] K.F. Graff, Wave Motion in Elastic Solids, Ohio State University Press, Columbus, Ohio, 1975.

[3] K. Ogata, Modern Control Engineering, Prentice Hall, Englewood Cliffs, NJ, 1970.

[4] S.H. Crandall, and W.D. Mark, Random Vibration in Mechanical Systems, Academic Press, N.Y., 1973.

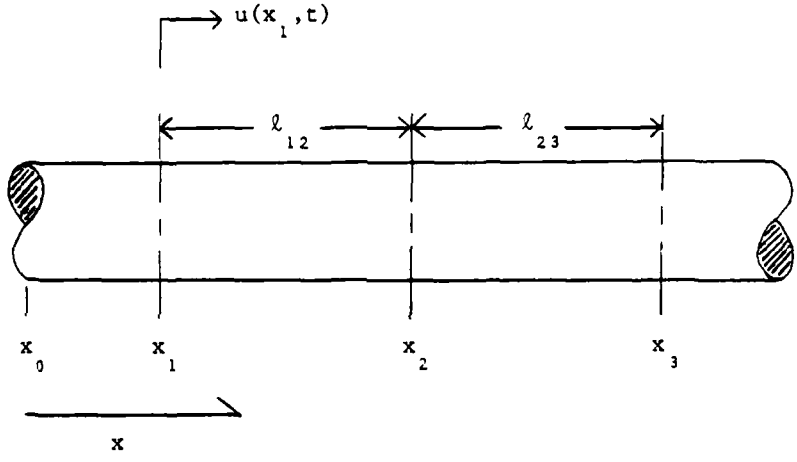

Fig. 1 Geometry of lattice substructure.

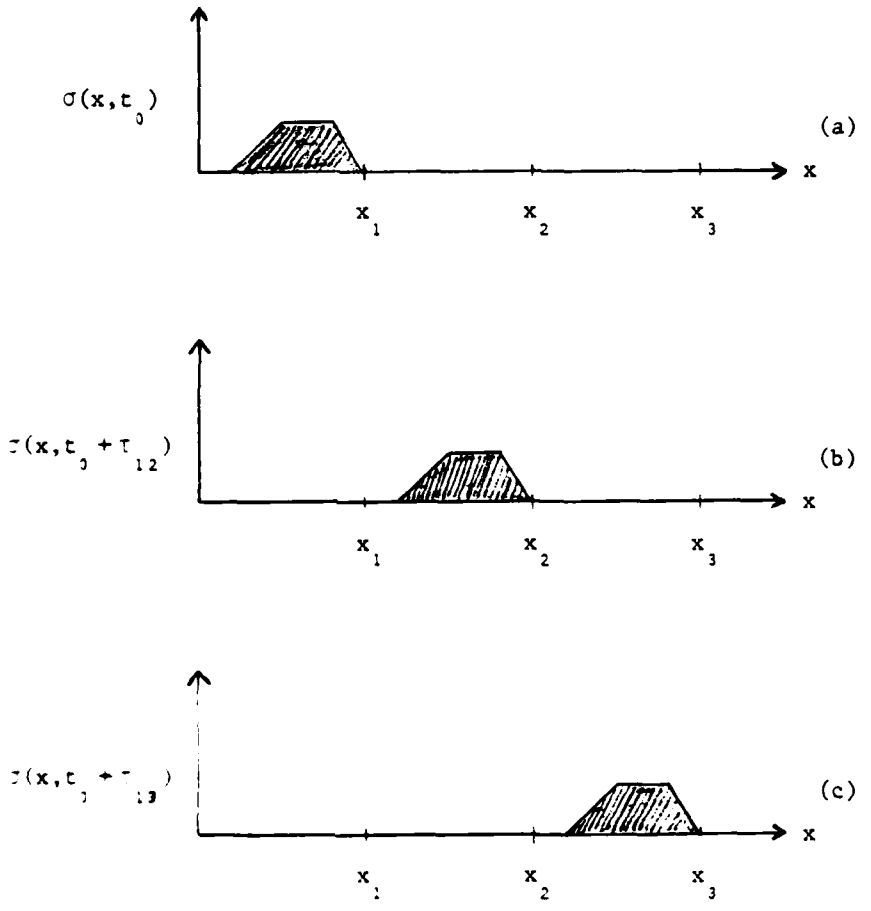

Fig. 2 Nondispersive stress wave propagation.

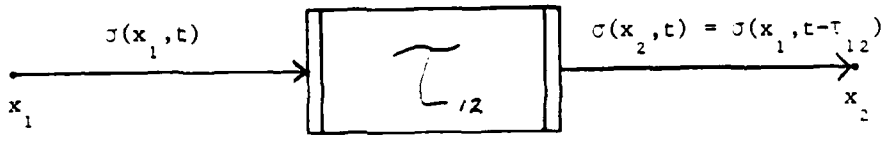

Fig. 3 Schematic of delay block.

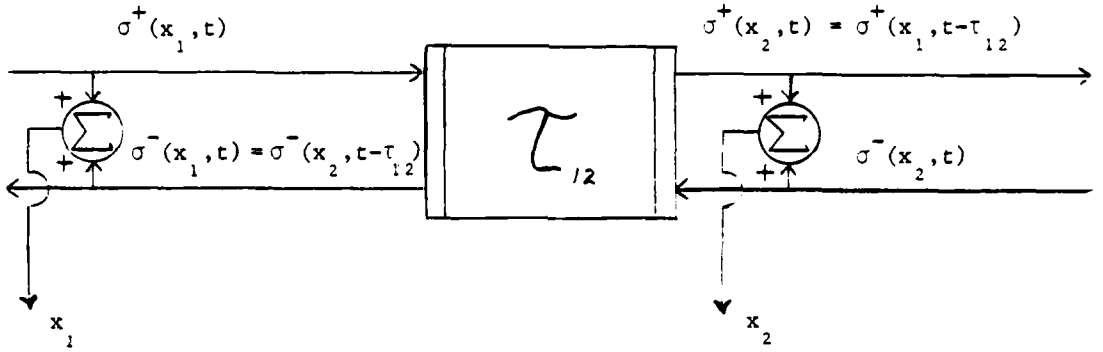

$$\sigma(x_1,t) = \sigma^+(x_1,t) + \sigma^-(x_1,t)$$

$$\sigma(x_2,t) = \sigma^+(x_2,t) + \sigma^-(x_2,t)$$

Fig. 4 Block diagram with superposition at cross sections.

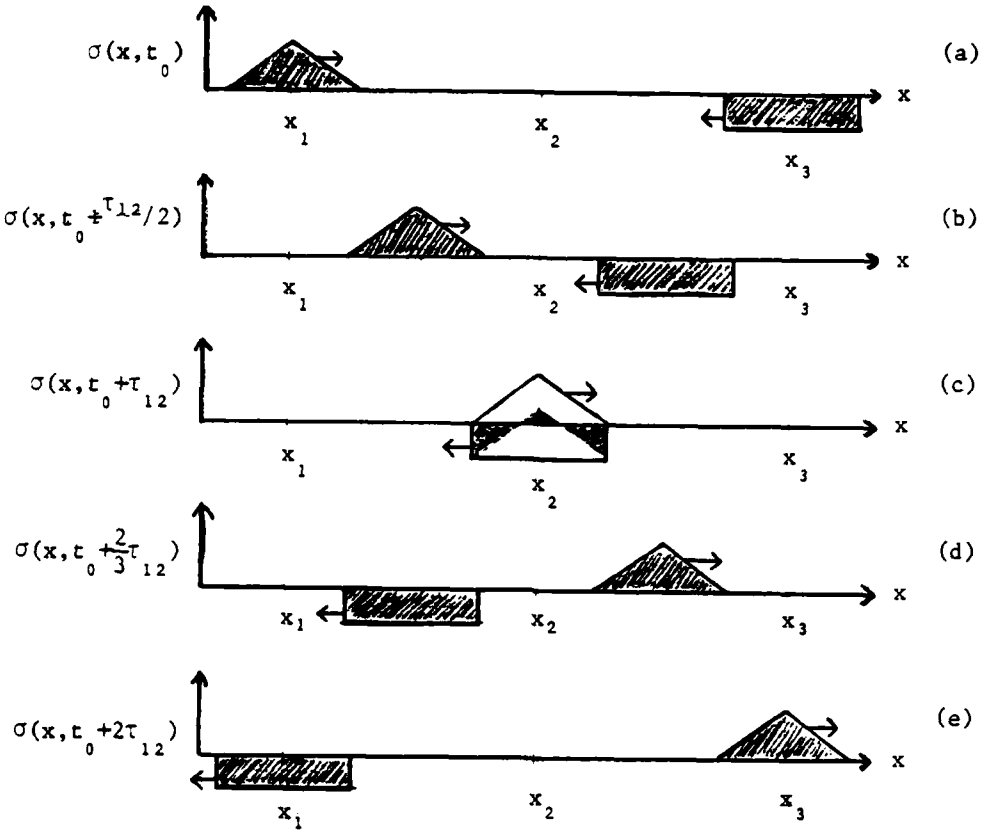

Fig. 5 Illustration of superposition.

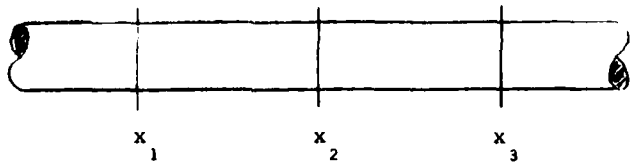

(a)

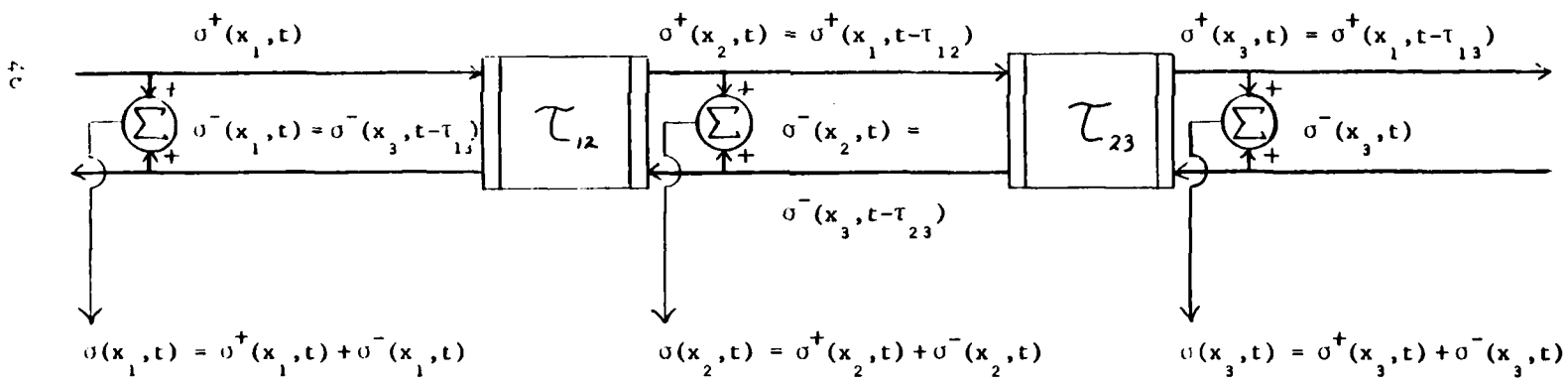

(b)

Fig. 6 (a) Lattice element and (b) its block diagram model.

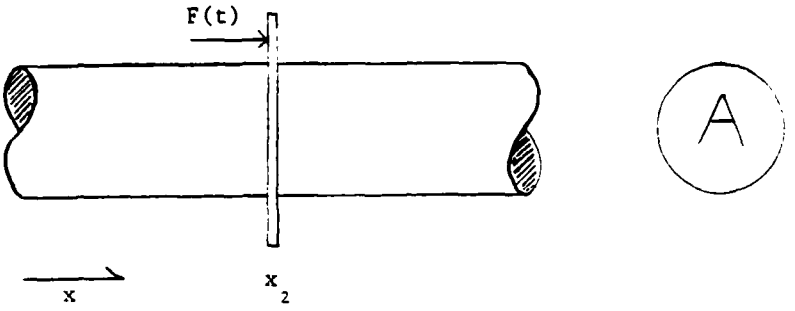

(a)

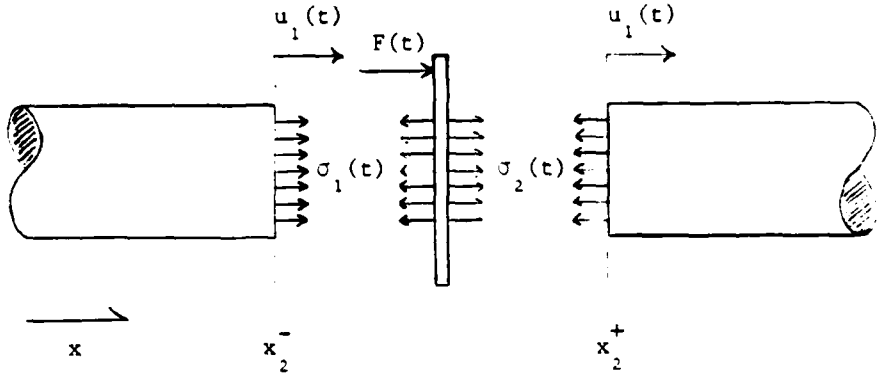

(b)

Fig. 7 (a) Idealized actuator-substructure assembly and (b) its free body diagram.

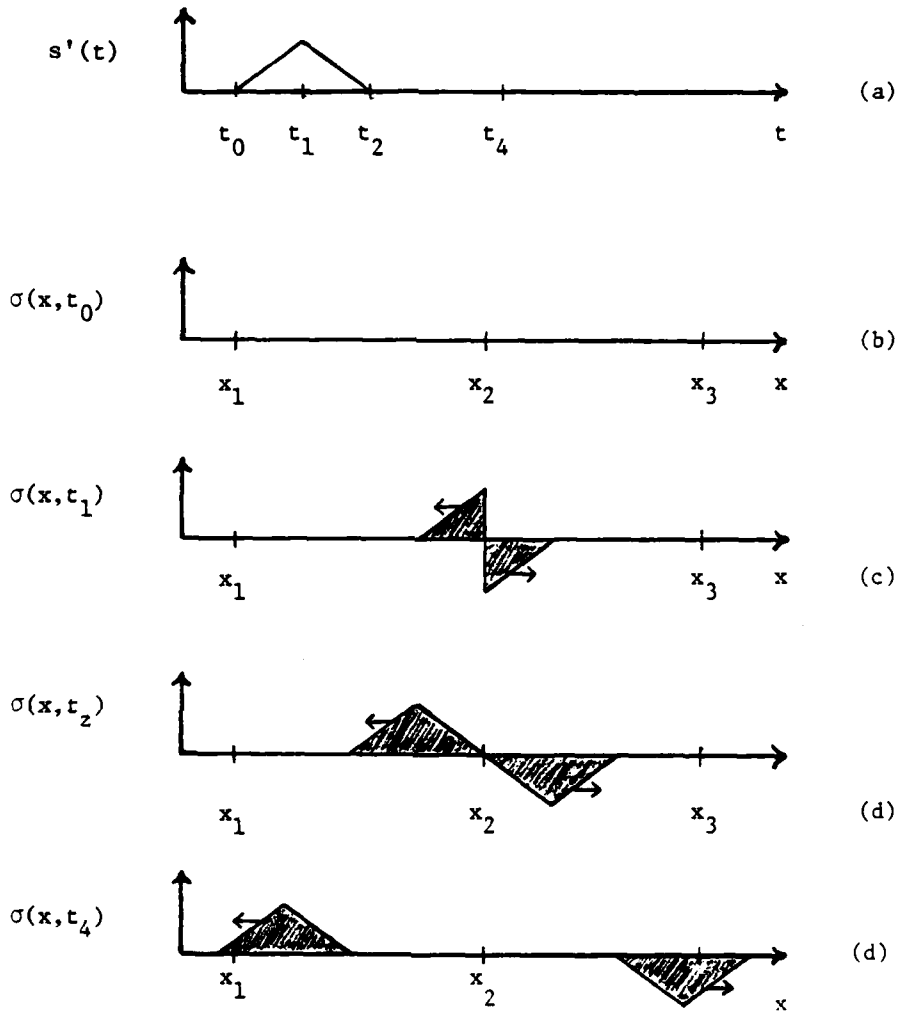

Fig. 8 Illustration of actuator output.

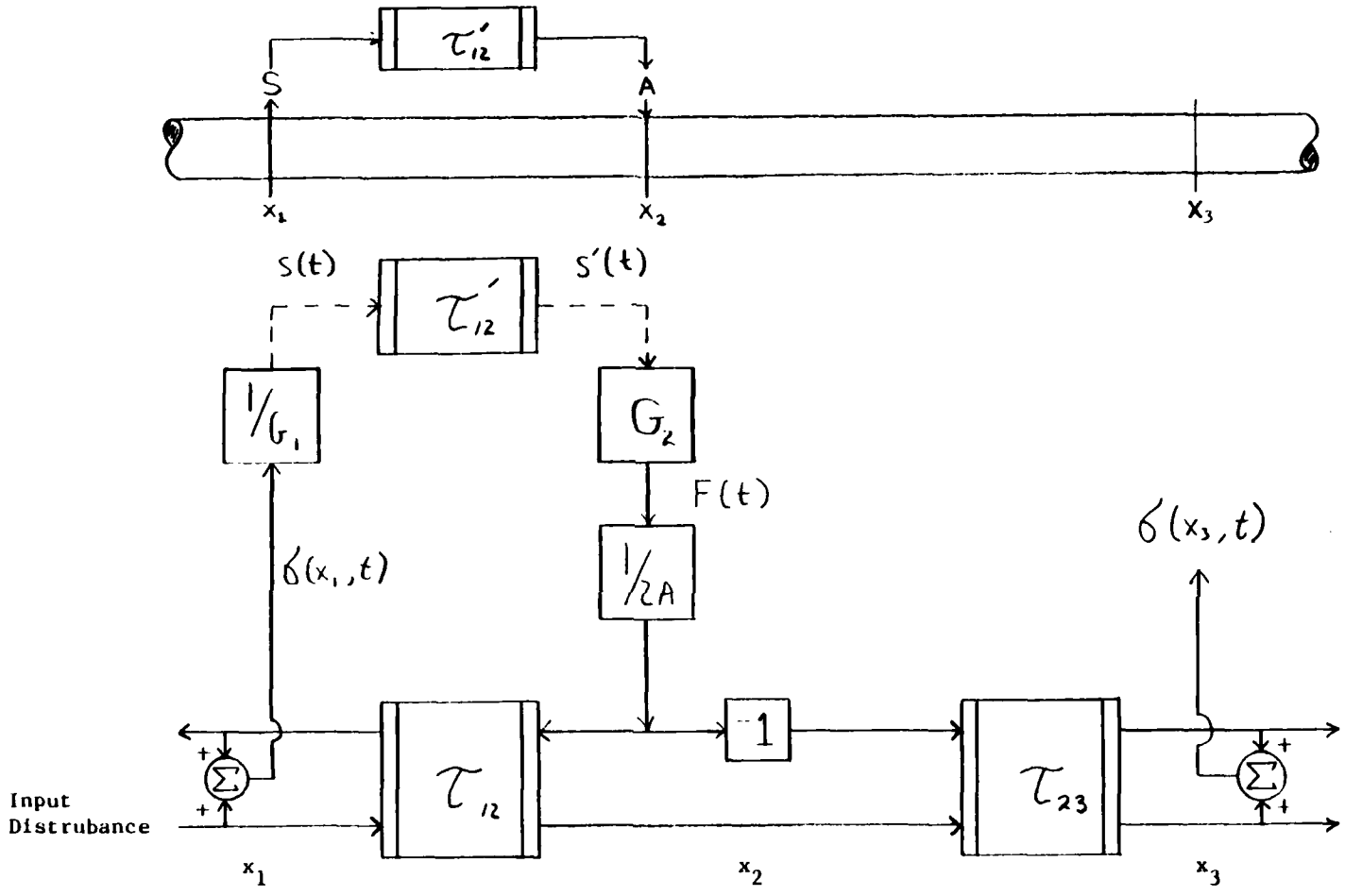

Fig. 9 Comprehensive block diagram.

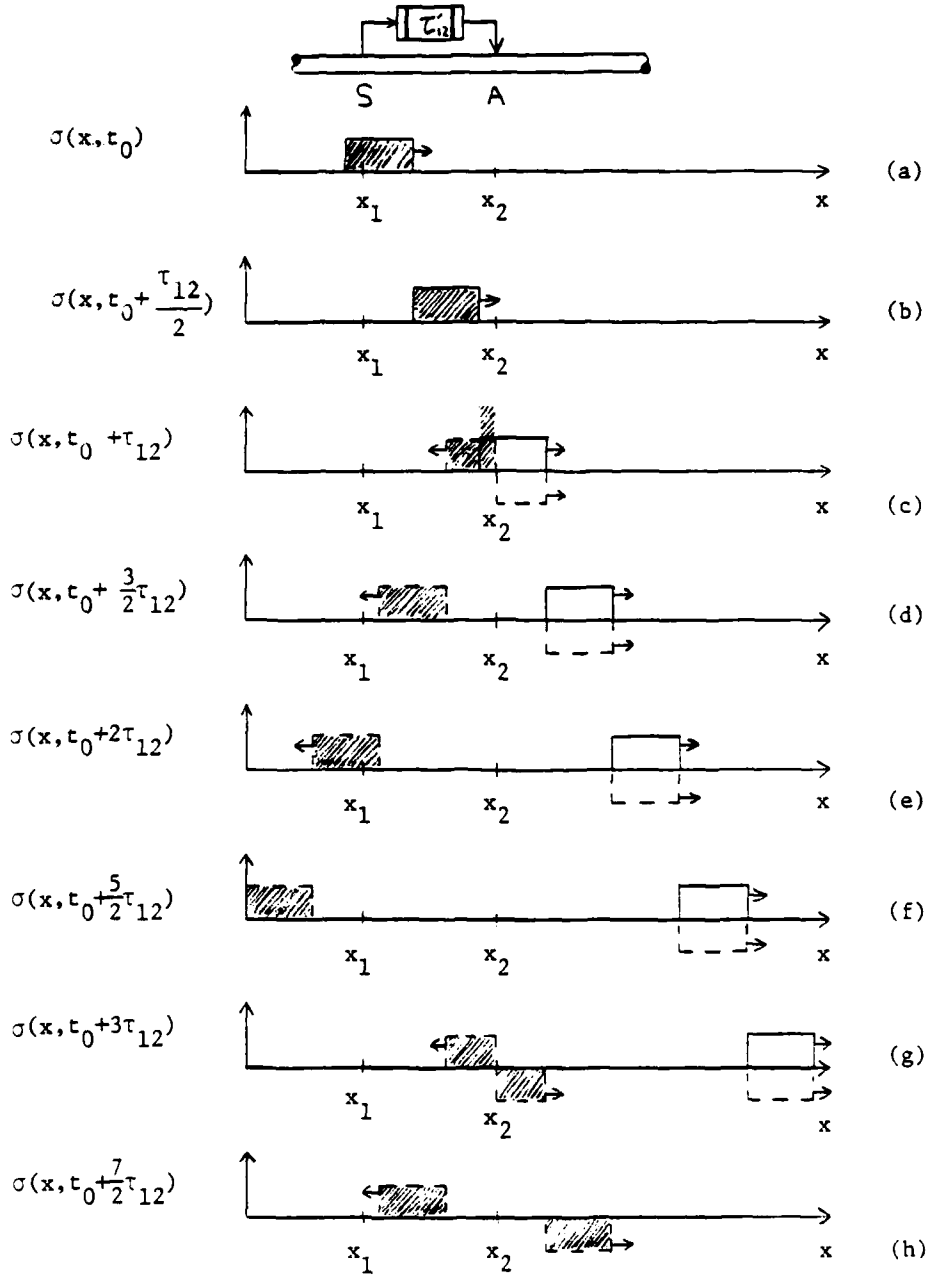

Fig. 10 Response of controlled substructure to single square wave input.

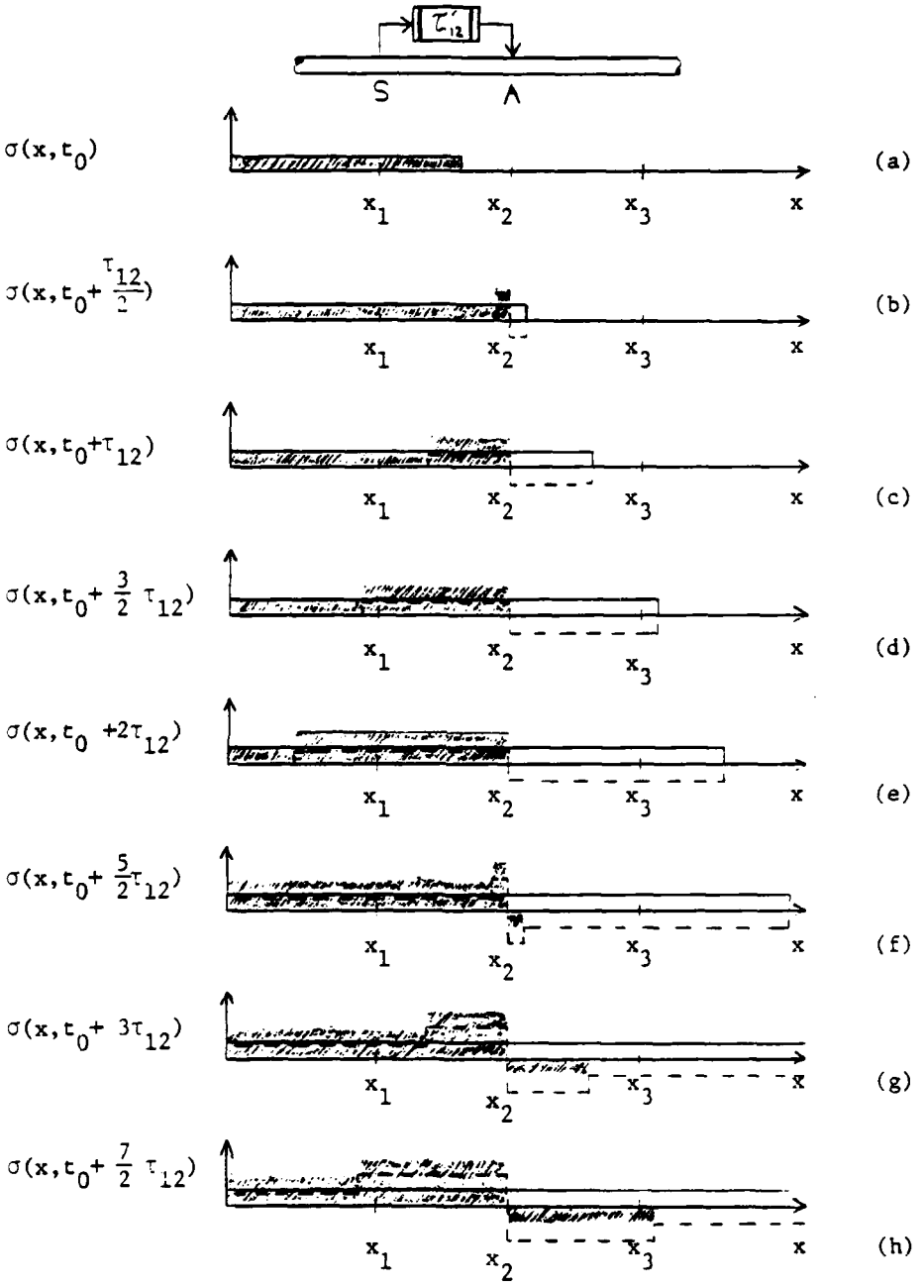

Fig. 11 Response of controlled substructure to step input.

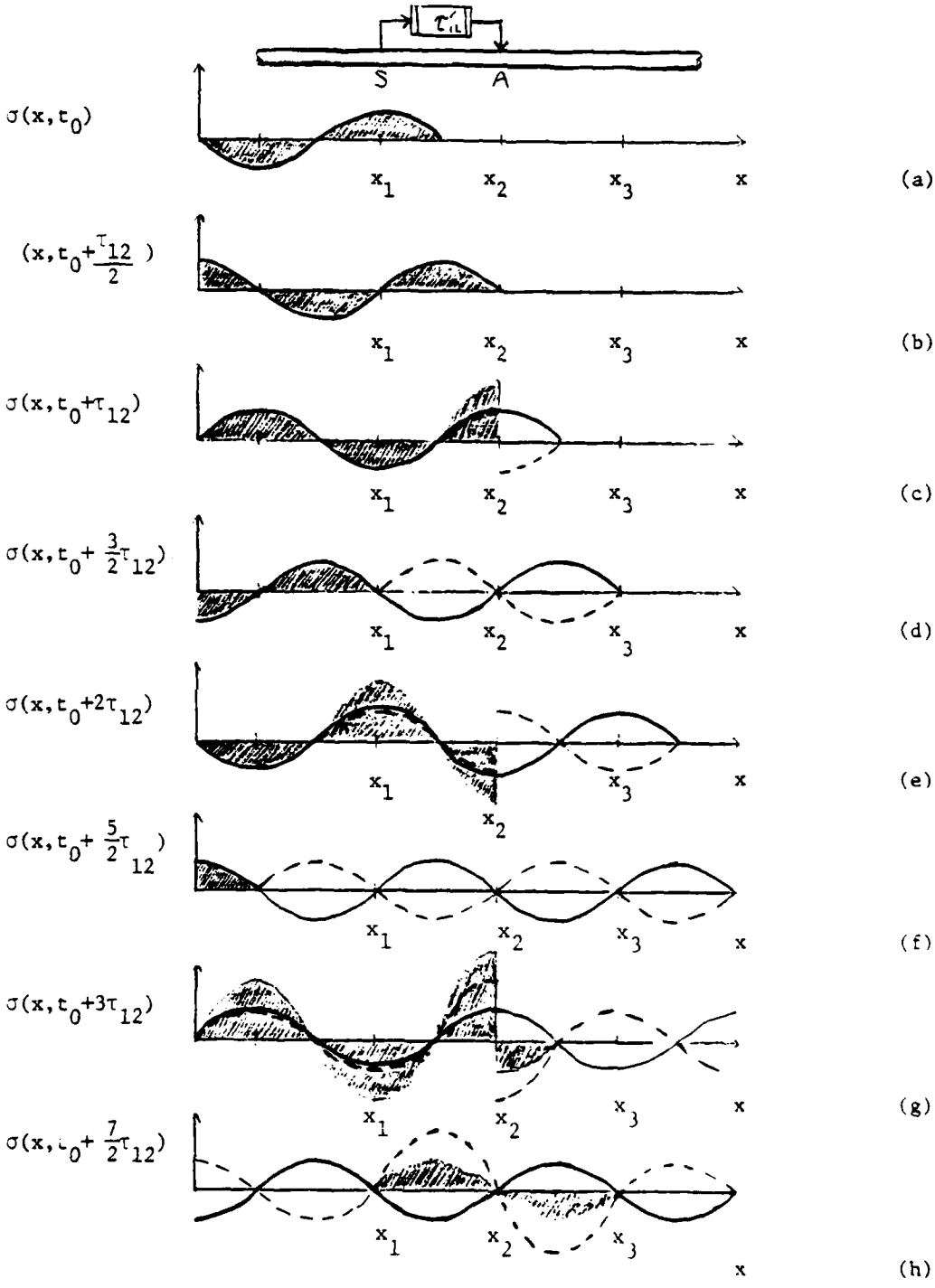

Fig. 12 Response of controlled substructure to step sinusoid input.

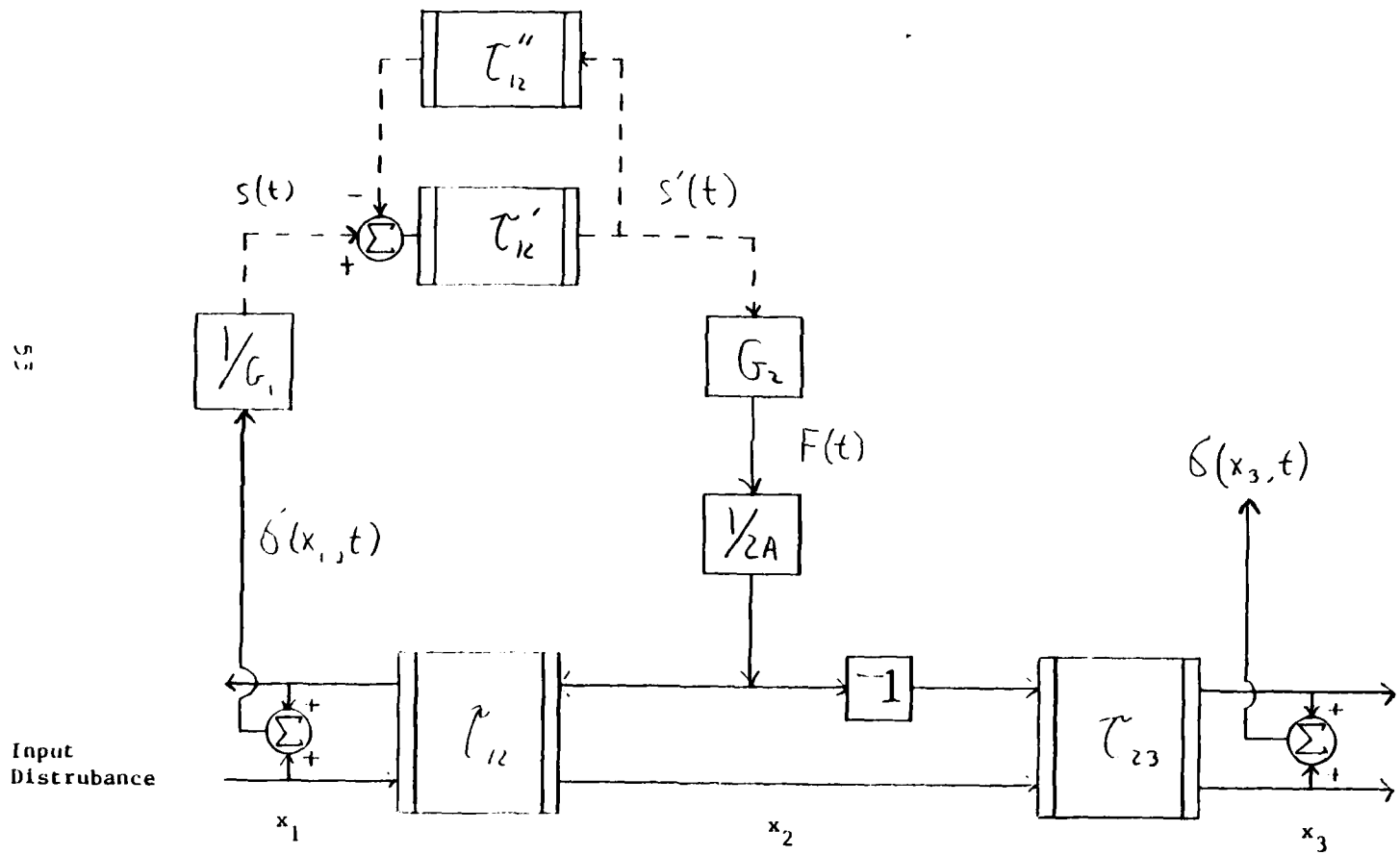

Fig. 13 Modified controller design.

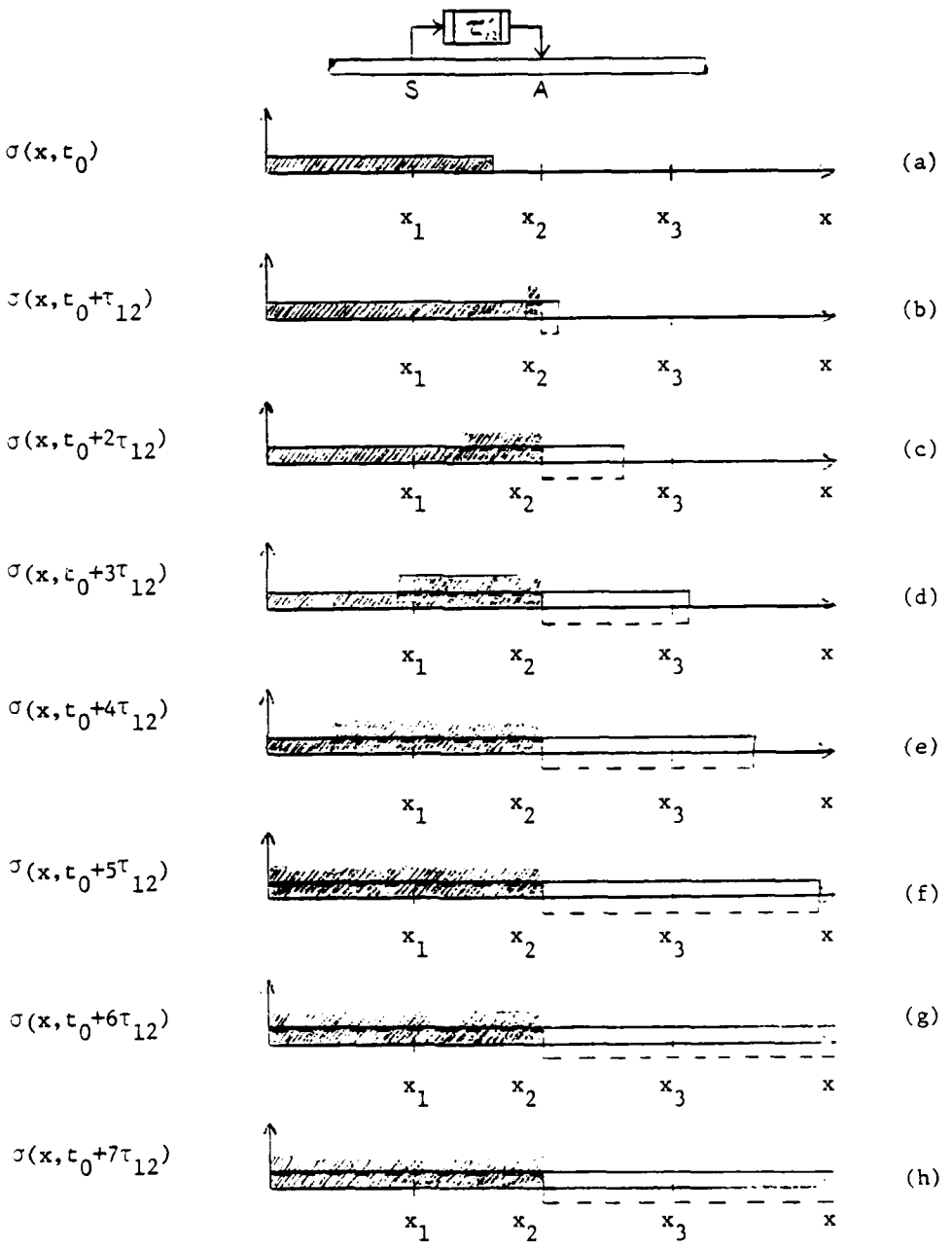

Fig. 14 Step response of system with modified controller.

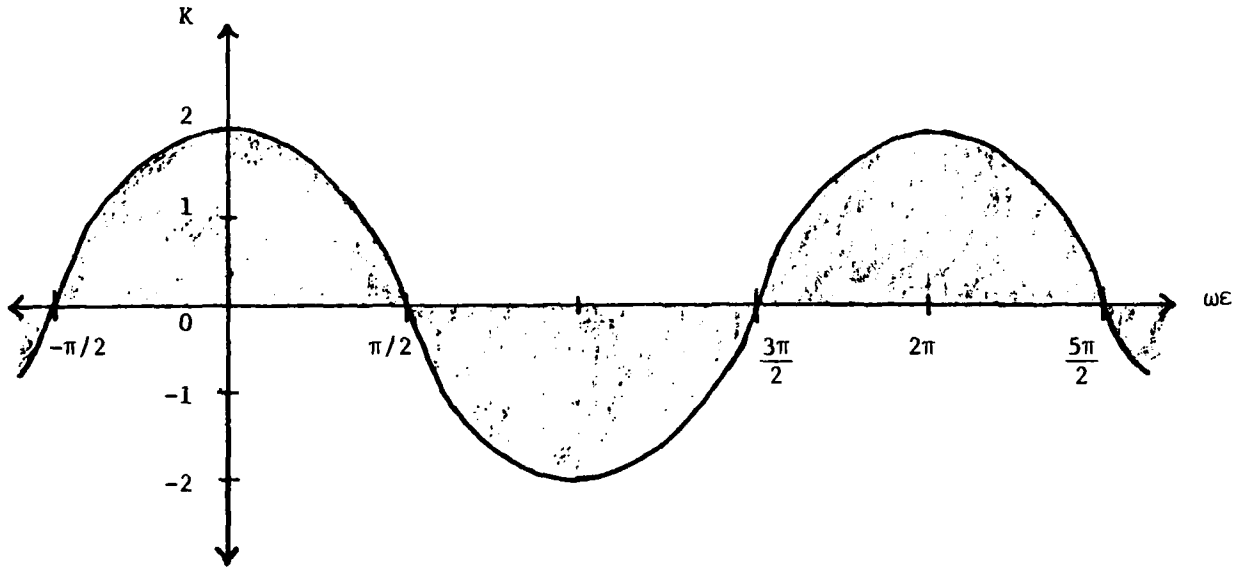

Fig. 15 Locus of parameter value in the K versus $\omega\varepsilon$ plane for which the system attenuates a sinusoidal input.

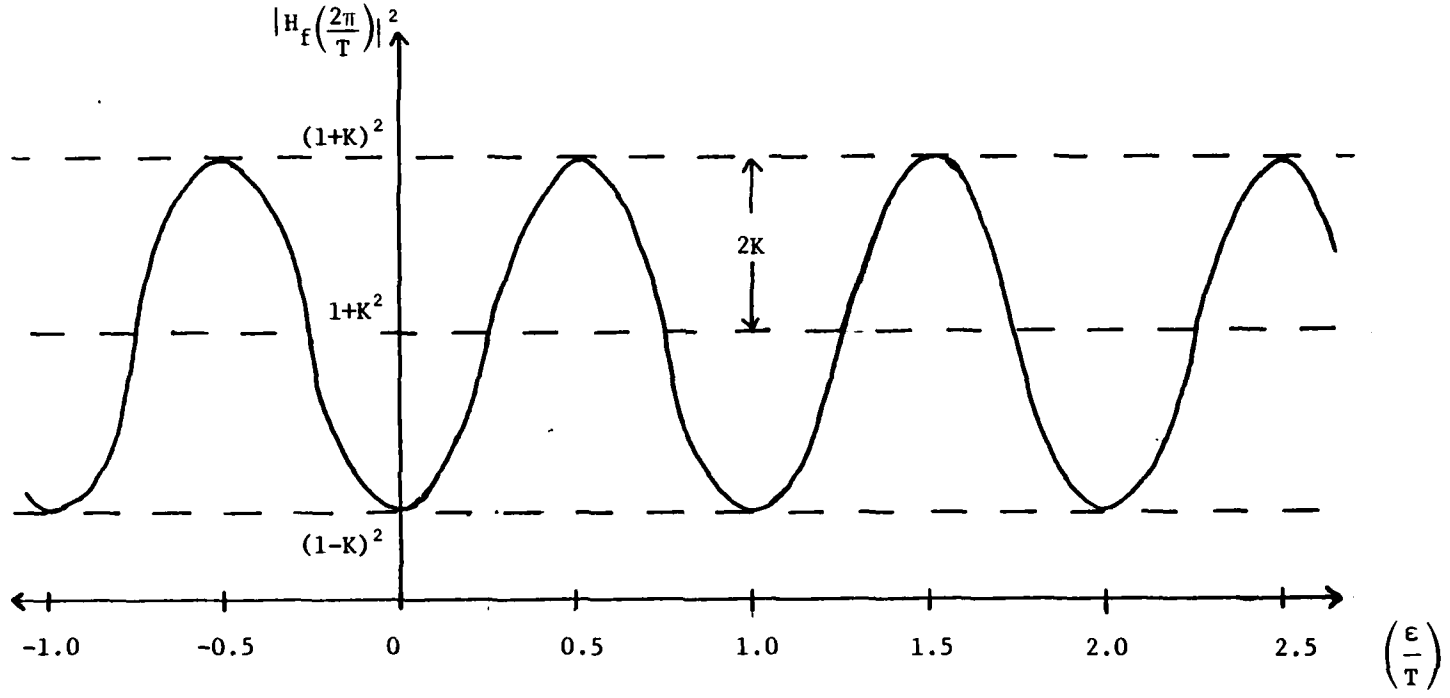

Fig. 16 Square of magnitude of transfer function for feedforward control of wave propagation in lattice substructure versus parameter $(\frac{\varepsilon}{T})$.

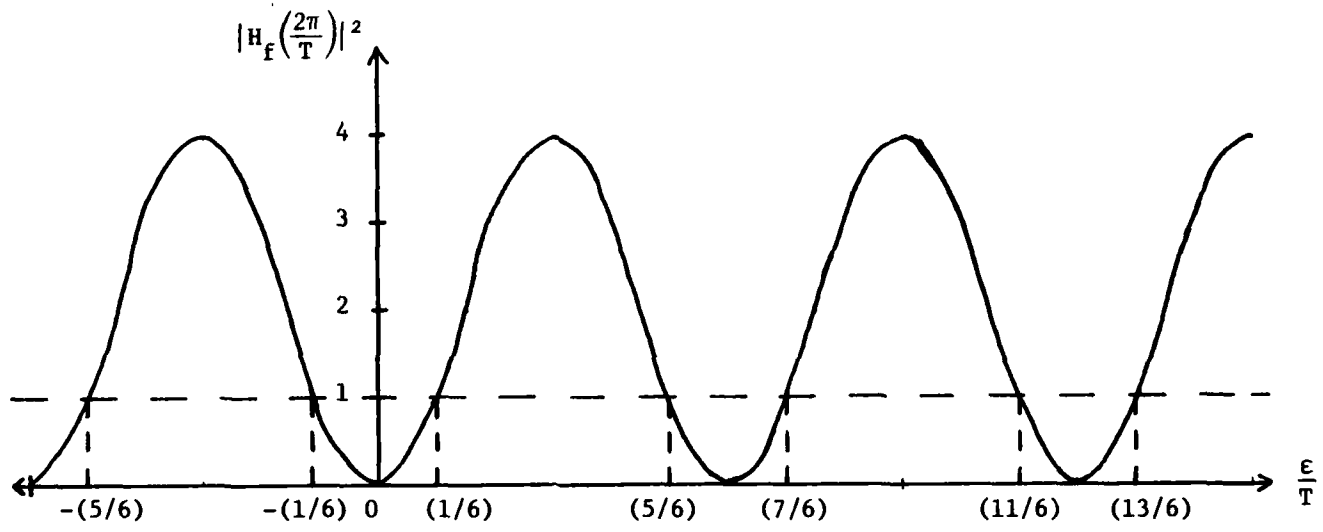

Fig. 17 Square of system transfer function magnitude for feedforward gain K equal to unity, versus parameter $\left(\frac{\varepsilon}{T}\right)$.

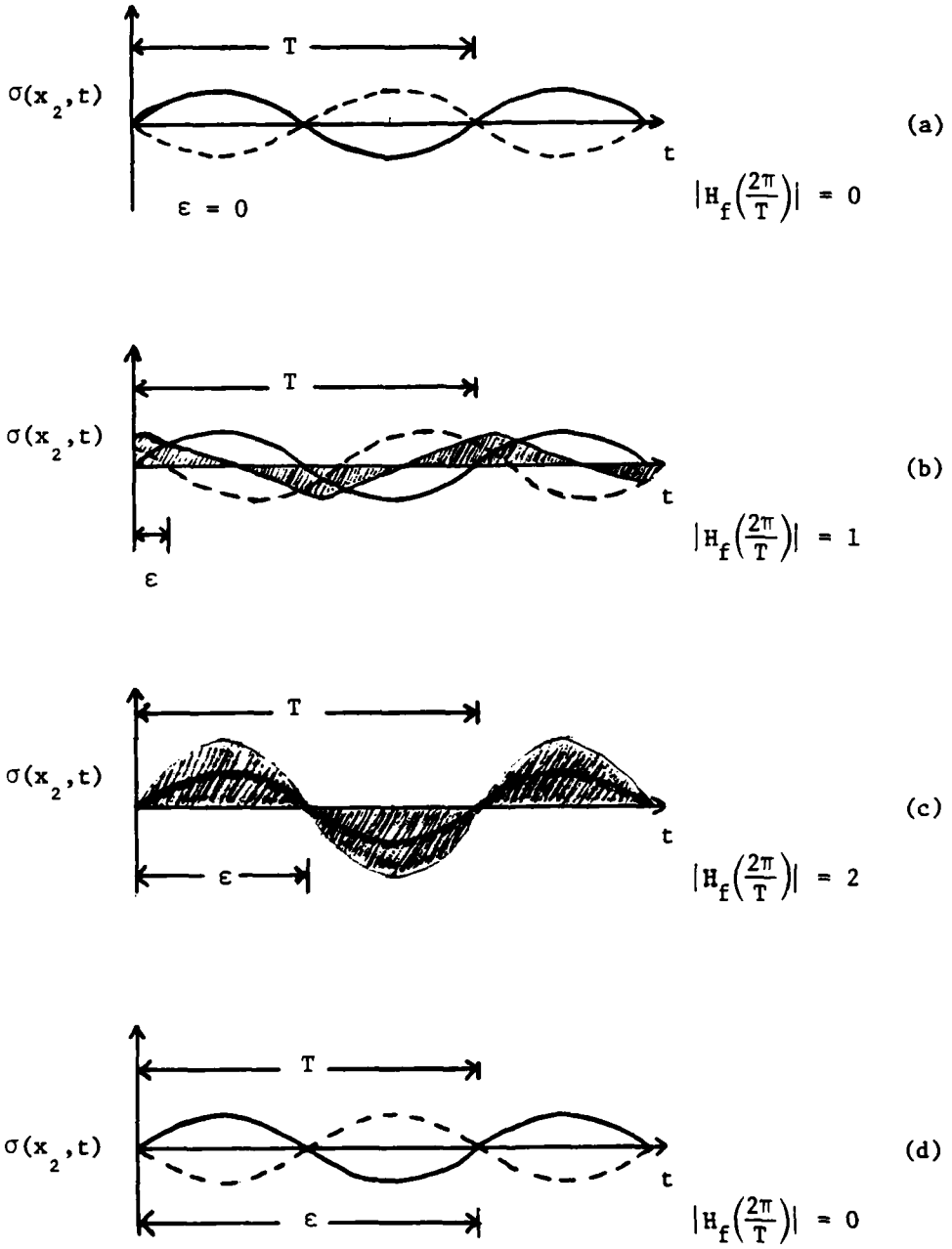

Fig. 18 Illustration of frequency dependence of transfer function magnitude for constant T and varying ε .

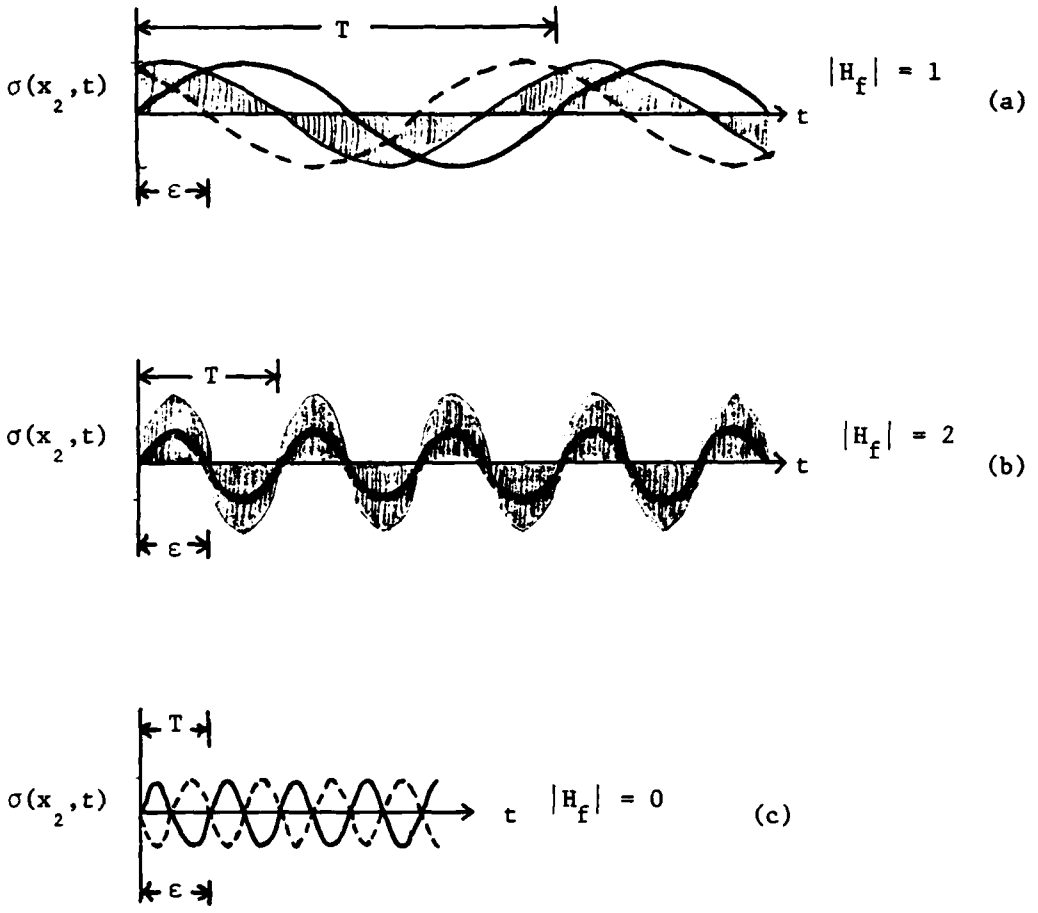

Fig. 19 Illustration of frequency dependence of transfer function magnitude for constant ε and varying T.

APPENDIX A

ANALYSES OF FEEDBACK CONTROL OF WAVE PROPAGATION IN STRUCTURES

The feedback control of wave propagation in lattice structures is considered in this appendix. Limitations of such a control scheme are illustrated and discussed.

The geometry of a one-dimensional lattice substructure, which is modelled as a thin rod, is shown in Fig. A-1. As shown, the coordinate x refers to the undisturbed location of a cross section of the substructure. Two sections of the substructure, separated by distance ℓ_{12}, are labelled as x_1 and x_2. A section to the right of x_2 is labelled as x_3. The section x_3 represents the location in the substructure to be protected from incoming stress disturbances by the feedback system.

In the feedback control scheme, a disturbance is assumed to originate from the left of x_1 and propagate through the substructure. A sensor measures the stress (or displacement or velocity) at cross section x_2, and the feedback system provides a force in the longitudinal direction at cross section x_2 through an actuator. The force provided by the actuator generates a rightwardly-propagating stress wave at x_1 whose instantaneous amplitude at x_1 is the exact negative of the stress sensed at x_2. The force provided by the actuator also generates a corresponding leftwardly-propagating stress wave at x_1 which is the negative of the rightwardly-propagating stress wave. (In this study, leftwardly-propagating waves are not reflected at the left boundary of the substructure.) The total response of the substructure is the superposition of the incoming stress wave

disturbance and the stress waves generated by the actuator.

Figs. A-2 and A-3 show the responses of the substructure under feedback control to an input single pulse disturbance and to an input step disturbance, respectively. The sensor S is located at x_2 and the actuator A is located at x_1. The feedback system is indicated by a block diagram containing -1 as the only entry. The transit time for wave propagation from x_1 to x_2 is τ_{12}. Figs. A-2 and A-3 show the stress distributions $\sigma(x,t)$ along the length of the substructure at equal time intervals for increasing time. The time interval shown corresponds to half the transit time τ_{12}. A rightwardly-propagating stress wave disturbance originates to the left of x_1. The stress distribution along the substructure is observed at time t_0, after the disturbance has passed location x_1 but before it has reached location x_2. Then, the stress distributions along the substructure at t_1, t_2,..., t_6, t_7 are shown.

In Figs. A-2 and A-3, the solid outlines represent the incoming stress disturbance and the dashed outlines represent the stress waves generated by the actuator. Also, the shaded portions represent the net, or physically realized magnitude of the stress waves in the substructure due to superposition of the incoming disturbance and the actuator-generated stress waves.

Figs. A-2a through A-2h show the responses of the substructure to a single pulse disturbance. The duration of the disturbance is assumed to be less than the transit time τ_{12}. Fig. A-2b shows the incoming disturbance just before it arrives at the sensor S. Fig. A-2c shows the incoming disturbance as it is just

passing S and the actuator is active in producing both a rightwardly-propagating wave and a leftwardly-propagating wave. Fig. A-2d shows the incoming disturbance after it has passed S and the actuator is not active. However, a negative pulse propagating to the right has been generated by the actuator. Fig. A-2e shows the actuator generating stress waves due to the negative actuator-generated rightwardly-propagating wave. This process continues indefinitely and an infinite sequence of identical pulses, with alternating sign and separated by τ_{12}, is sent to the right of location x_2. Thus, if a point to the right of x_2 (that is, point x_3) is to be protected from stress disturbances by the feedback system, the feedback system actually worsens the situation by generating more pulses towards the point of interest.

Figs. A-3a through A-3h show the responses of the substructure to a step disturbance. Fig. A-3a shows the incoming disturbance just before it arrives at the sensor S. Fig. A-3b shows the leading edge of the incoming disturbance has just passed S and the actuator is active in producing both a rightwardly-propagating wave and a leftwardly-propagating wave. The actuator-generated rightwardly-propagating wave cancels the portion of the incoming disturbance that overlaps with it. Fig. A-3c shows the leading edge of the actuator-generated rightwardly-propagating wave has passed the sensor S and has cancelled the incoming disturbance at S. Because there is no longer any stress at S, the actuator is not active. Thus, the incoming disturbance arriving at the actuator A passes unaltered as shown in Figs. A-3d and A-3e. Fig. A-3f shows the leading

edge of the unaltered incoming disturbance has just passed the sensor S and the actuator is active again. This process continues indefinitely and an infinite sequence of identical pulses, each with duration equal to the transit time τ_{12} and each also separated by τ_{12}, is sent to the right of location x_2. Thus, if a point to the right of x_2 (that is, point x_3) is to be protected from stress disturbances by the feedback system, the feedback system does not remove all of the step stress disturbance, but does prevent segments of the input step from reaching the point of interest. The penalty is that segments of leftwardly-propagating waves to the left of x_1 have double the amplitude of the incoming disturbance.

To summarize, the feedback control of wave propagation in lattice substructures as described here has significant limitations. For short input pulse disturbances as shown in Fig. A-2, an infinite sequence of pulses of alternating sign is generated to the right of location x_2. For long input pulse disturbances as shown in Fig. A-3, only a portion of the disturbance is prevented from reaching a location to the right of x_2 (that is, point x_3). However, as shown in Figs. A-2 and A-3, this control system does not appear to cause system instability because the stress amplitudes are always limited. Nevertheless, feedback control may still be useful as a part of a total control scheme for the control of wave propagation in lattice structures.

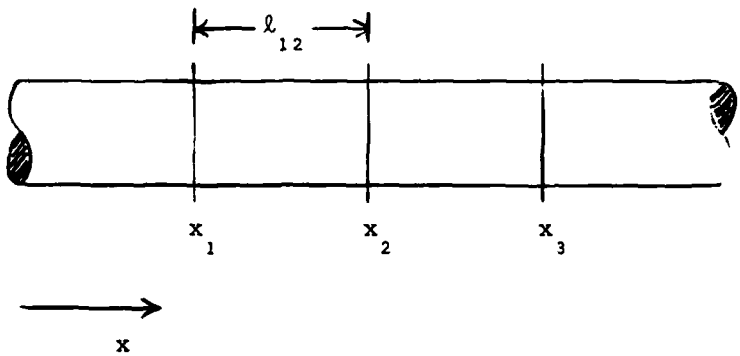

Fig. A-1 Geometry of structure considered.

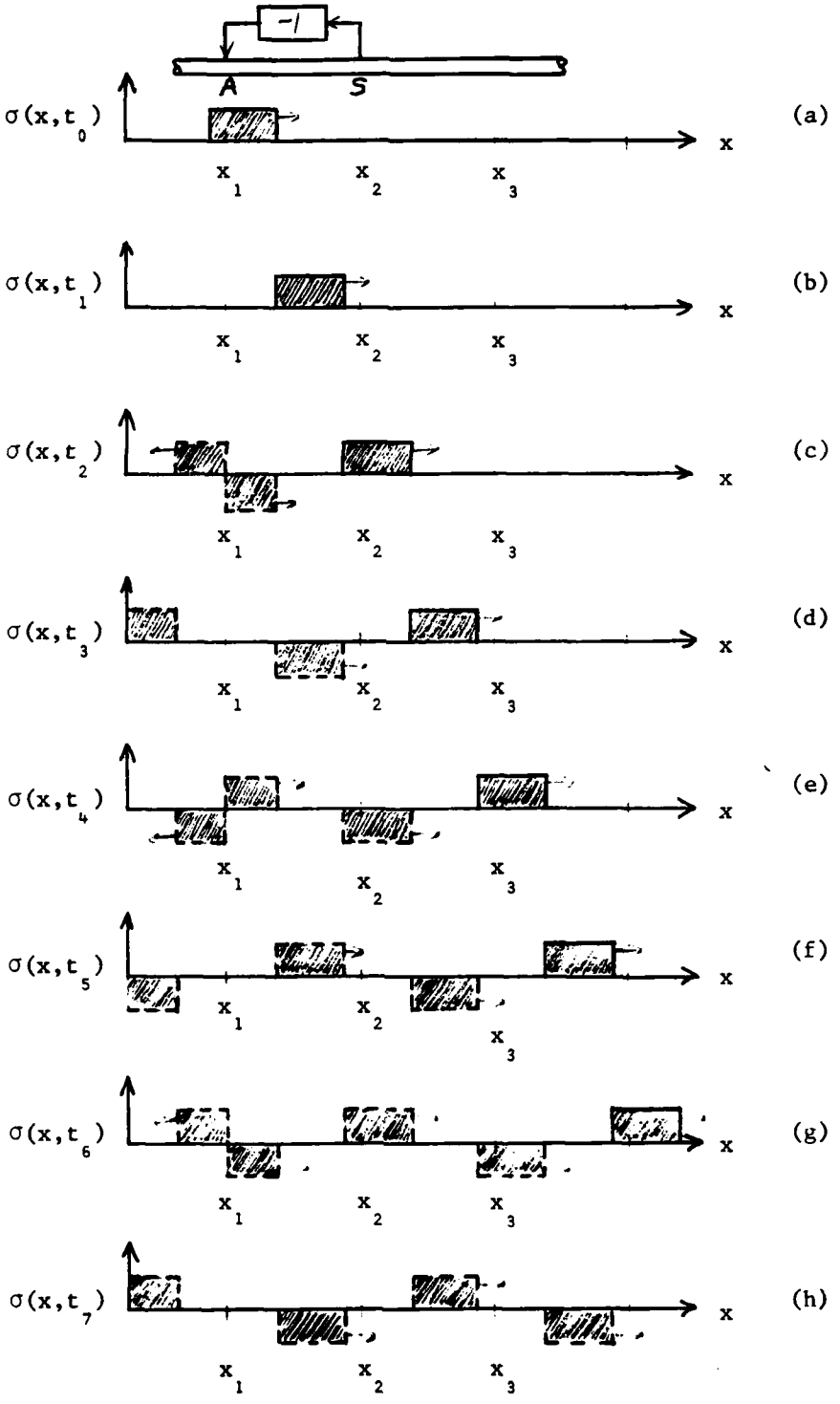

Fig. A-2 Response of structure under feedback control to input single pulse disturbance.

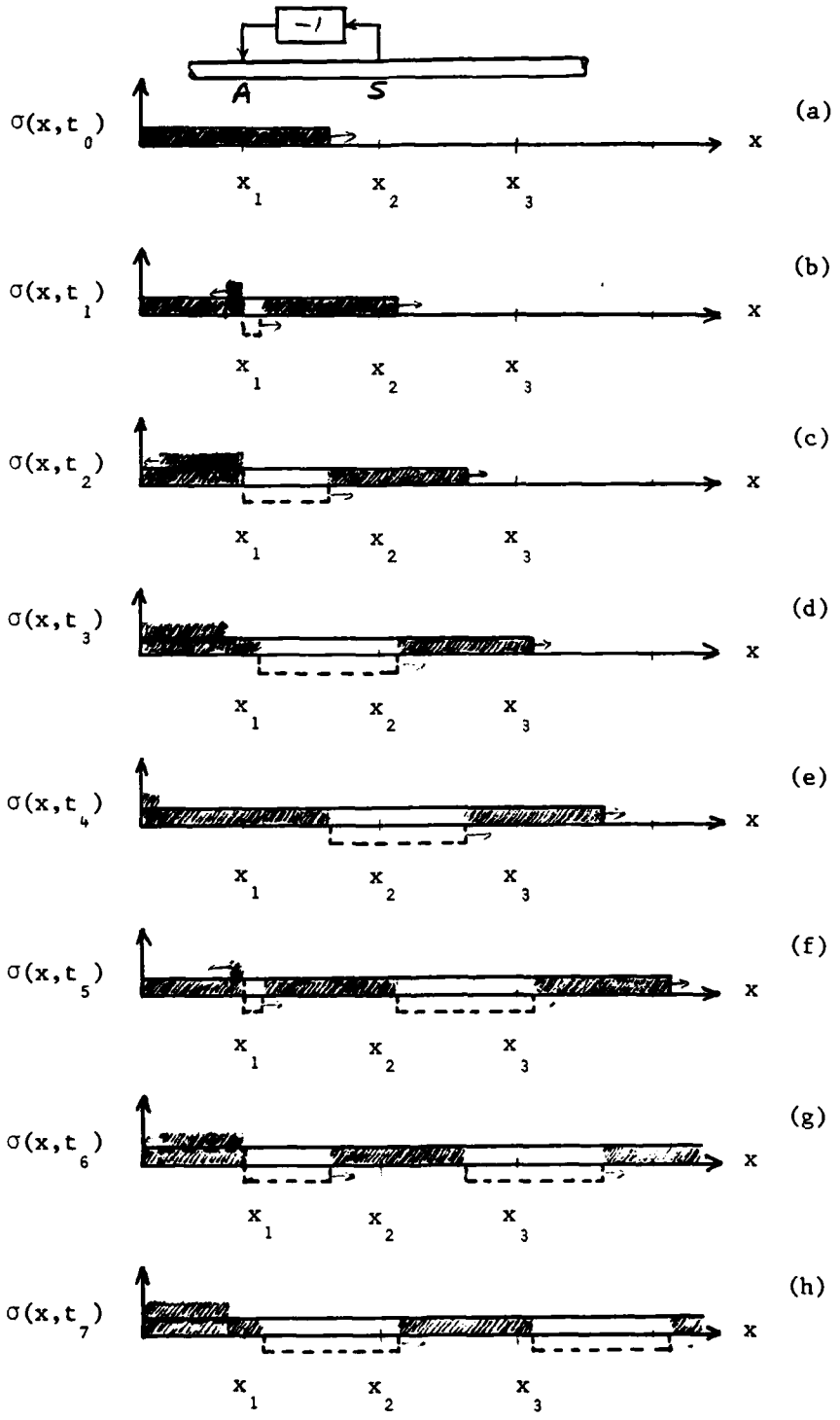

Fig. A-3 Response of structure under feedback control to input step disturbance.

APPENDIX B

IMPULSE RESPONSE AND TRANSFER FUNCTION FOR WAVE PROPAGATION FEEDFORWARD CONTROL

The impulse response and the transfer function for the feedforward control of wave propagation in structures are considered in this Appendix.

In general, a linear system can be characterized by its impulse response $h(t)$ or its transfer function $H(\omega)$ as shown in Fig. B-1 [4]. (The transfer function is also called the frequency response.) For an input $x(t)$, where t denotes time, the output $y(t)$ can be obtained via $h(t)$ as [4]

$$y(t) = \int_{-\infty}^{\infty} x(\tau)\, h(t-\tau)\, d\tau \tag{B.1}$$

where τ is a variable of integration. For an input $X(\omega)$, where ω denotes radian frequency, the output $Y(\omega)$ can be obtained via $H(\omega)$ as [4]

$$Y(\omega) = H(\omega)\, X(\omega) \tag{B.2}$$

Furthermore, the impulse response and the transfer function are related as [4]

$$H(\omega) = \int_{-\infty}^{\infty} h(t)\ e^{-i\omega t}\, dt \tag{B.3}$$

where i denotes $\sqrt{-1}$.

Fig. B-2 shows a schematic of the feedforward control of

wave propagation in structures. The substructure is characterized by a time delay of τ_{12} . The feedforward controller is characterized by a time delay of τ_{12}' and an amplification factor K. (Waves may be generated at the actuator and propagate back along the structure toward the sensor. However, it is assumed in this Appendix that these particular waves are ignored by the sensor. Also, it is noted that dispersion and attenuation are not considered in the model shown in Fig. B-2.) The output of the feedforward control system is formed by subtracting the output of the feedforward controller from the output of the substructure as indicated in Fig. B-2.

Considering an input impulse $\delta(t)$ into the feedforward control system shown in Fig. B-2, the impulse response $h_f(t)$ of the feedforward control system can be written as

$$h_f(t) = \delta(t-\tau_{12}) - K\delta(t-\tau_{12}') \tag{B.4}$$

where δ is the Dirac delta function [4].

Eqn. (B.4) shows that the output of the feedforward control system is formed by subtracting the output of the feedforward controller, which is the input impulse time-delayed by τ_{12}' and scaled by K, from the output of the substructure only, which is the input impulse time-delayed by τ_{12} and scaled by unity.

Then, the transfer function $H_f(\omega)$ of the feedforward control system shown in Fig. B-2 can be obtained from $h_f(t)$ via eqn. (B.3) as

$$H_f(\omega) = \int_{-\infty}^{\infty} h_f(t)\, e^{-i\omega t}\, dt \tag{B.5}$$

Substituting eqn. (B.4) into eqn. (B.5) gives

$$H_f(\omega) = \int_{-\infty}^{\infty} \left[\delta(t-\tau_{12}) - K\delta(t-\tau_{12}')\right] \; e^{-i\omega t}\, dt \qquad (B.6)$$

From the properties of Dirac delta function, eqn. (B.6) can be integrated to give [4]

$$H_f(\omega) = e^{-i\omega\tau_{12}} - Ke^{-i\omega\tau_{12}'} \qquad (B.7)$$

Eqn. (B.7) gives the transfer function $H_f(\omega)$ of the feedforward control system shown in Fig. B-2. As shown in eqn. (B.7), the transfer funtion is a complex function. The magnitude of the transfer function will be discussed.

The square of the magnitude of $H_f(\omega)$ can be obtained from [4]

$$|H_f(\omega)|^2 = H_f(\omega)H_f(-\omega) \qquad (B.8)$$

where $|H_f(\omega)|^2$ denotes the square of the magnitude of $H_f(\omega)$ and $H_f(-\omega)$ denotes the complex conjugate of $H_f(\omega)$.

The complex conjugate of $H_f(\omega)$ can be obtained from eqn. (B.7) as

$$H_f(-\omega) = e^{i\omega\tau_{12}} - Ke^{i\omega\tau_{12}'} \qquad (B.9)$$

Substituting eqns. (B.7) and (B.9) into eqn. (B.8) gives

$$|H_f(\omega)|^2 = \left(e^{-i\omega\tau_{12}} - Ke^{-i\omega\tau_{12}'}\right)\left(e^{i\omega\tau_{12}} - Ke^{i\omega\tau_{12}'}\right) \qquad (B.10)$$

Eqn. (B.10) can be expanded as

$$|H_f(\omega)|^2 = e^{-i\omega\tau_{12} + i\omega\tau_{12}} - Ke^{-i\omega\tau_{12} + i\omega\tau_{12}'}$$

$$- Ke^{-i\omega\tau_{12}' + i\omega\tau_{12}} + K^2 e^{-i\omega\tau_{12}' + i\omega\tau_{12}'} \qquad (B.11)$$

Eqn. (B.11) can be simplified as

$$|H_f(\omega)|^2 = 1 - Ke^{i\omega(\tau_{12}' - \tau_{12})} - Ke^{-i\omega(\tau_{12}' - \tau_{12})} + K^2 \qquad (B.12)$$

The second and third terms on the right-hand side of eqn. (B.12) are complex conjugates of each other. When added, the imaginary parts of these two terms cancel. Thus, eqn. (B.12) becomes

$$|H_f(\omega)|^2 = 1 - 2K\cos\left[\omega(\tau_{12}' - \tau_{12})\right] + K^2 \qquad (B.13)$$

Defining

$$\tau_{12}' - \tau_{12} = \varepsilon \qquad (B.14)$$

where ε denotes the difference in time delays between the feedforward controller and the substructure, eqn. (B.13) can be rewritten as

$$|H_f(\omega)|^2 = 1 - 2K\cos(\omega\varepsilon) + K^2 \qquad (B.15)$$

Eqn. (B.15) gives the square of the magnitude of the transfer function for feedforward control of wave propagation in

the simple structures under consideration. Eqn. (B.15) is plotted in Fig. B-3 versus the parameter ($\omega\varepsilon$).

To summarize, the eqn. (B.15) and Fig. B-3 account for the general case where the time delay in the feedforward controller exceeds the time delays in the substructure by ε and also where the feedforward amplification is K, as shown in Fig. B-2. Fig. B-3 shows that the magnitude of the transfer function is periodic in $\omega\varepsilon$. Thus, when $\omega\varepsilon$ is increased (or decreased) by 2π, the transfer function magnitude repeats itself. Also, for a given ω, a positive ε and a negative ε of the same magnitude produce the same transfer function magnitude. Furthermore, Fig. B-3 shows that for any value of ε the magnitude of the transfer function has the least possible value when K equals unity. Finally, because the transfer function magnitude as shown in Fig. B-3 is frequency dependent, the feedforward control system response due to certain frequencies (for constant ε) is enhanced while tnat from other frequencies is diminished.

Eqn. (B.10) can be expanded as

$$|H_f(\omega)|^2 = e^{-i\omega\tau_{12} + i\omega\tau_{12}} - Ke^{-i\omega\tau_{12} + i\omega\tau_{12}'}$$

$$- Ke^{-i\omega\tau_{12}' + i\omega\tau_{12}} + K^2 e^{-i\omega\tau_{12}' + i\omega\tau_{12}'} \qquad (B.11)$$

Eqn. (B.11) can be simplified as

$$|H_f(\omega)|^2 = 1 - Ke^{i\omega(\tau_{12}' - \tau_{12})} - Ke^{-i\omega(\tau_{12}' - \tau_{12})} + K^2 \qquad (B.12)$$

The second and third terms on the right-hand side of eqn. (B.12) are complex conjugates of each other. When added, the imaginary parts of these two terms cancel. Thus, eqn. (B.12) becomes

$$|H_f(\omega)|^2 = 1 - 2K\cos\left[\omega(\tau_{12}' - \tau_{12})\right] + K^2 \qquad (B.13)$$

Defining

$$\tau_{12}' - \tau_{12} = \varepsilon \qquad (B.14)$$

where ε denotes the difference in time delays between the feedforward controller and the substructure, eqn. (B.13) can be rewritten as

$$|H_f(\omega)|^2 = 1 - 2K\cos(\omega\varepsilon) + K^2 \qquad (B.15)$$

Eqn. (B.15) gives the square of the magnitude of the transfer function for feedforward control of wave propagation in

the simple structures under consideration. Eqn. (B.15) is plotted in Fig. B-3 versus the parameter ($\omega\varepsilon$).

To summarize, the eqn. (B.15) and Fig. B-3 account for the general case where the time delay in the feedforward controller exceeds the time delays in the substructure by ε and also where the feedforward amplification is K, as shown in Fig. B-2. Fig. B-3 shows that the magnitude of the transfer function is periodic in $\omega\varepsilon$. Thus, when $\omega\varepsilon$ is increased (or decreased) by 2π, the transfer function magnitude repeats itself. Also, for a given ω, a positive ε and a negative ε of the same magnitude produce the same transfer function magnitude. Furthermore, Fig. B-3 shows that for any value of ε the magnitude of the transfer function has the least possible value when K equals unity. Finally, because the transfer function magnitude as shown in Fig. B-3 is frequency dependent, the feedforward control system response due to certain frequencies (for constant ε) is enhanced while that from other frequencies is diminished.

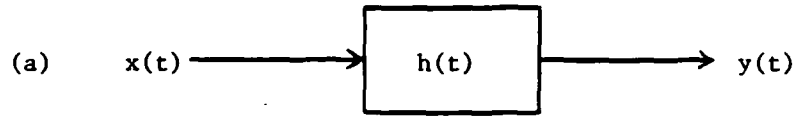

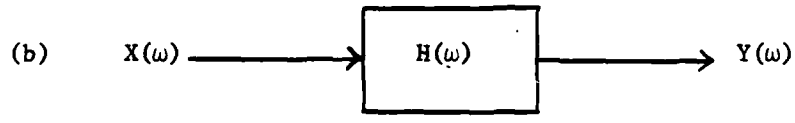

Fig. B-1 Linear system represented by its (a) impulse response h(t) and (b) transfer function H(ω).

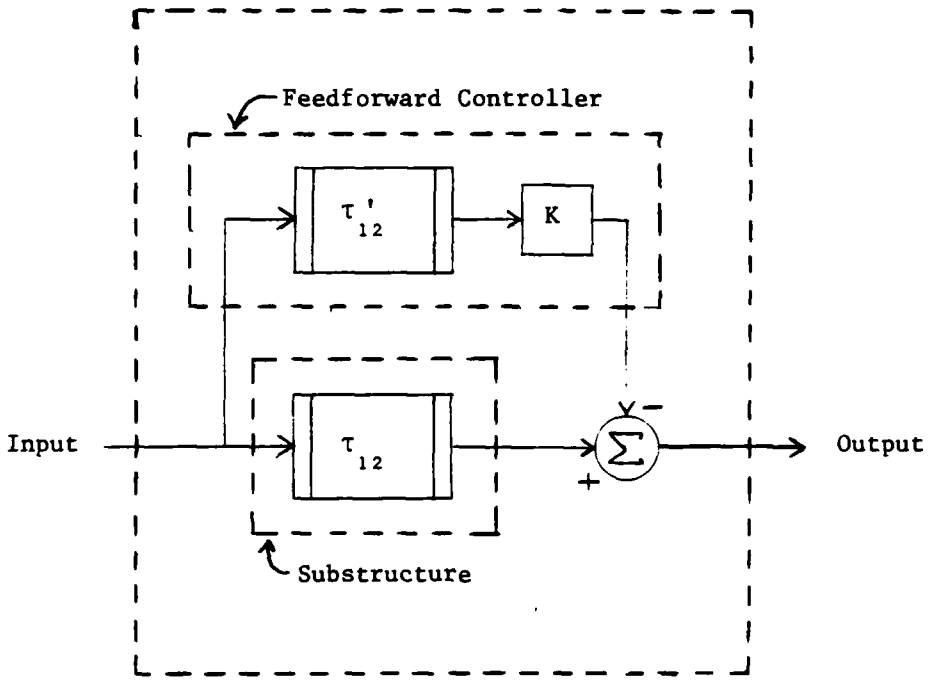

Feedforward Control System

Fig. B-2 Schematic of feedforward control of wave propagation in structures.

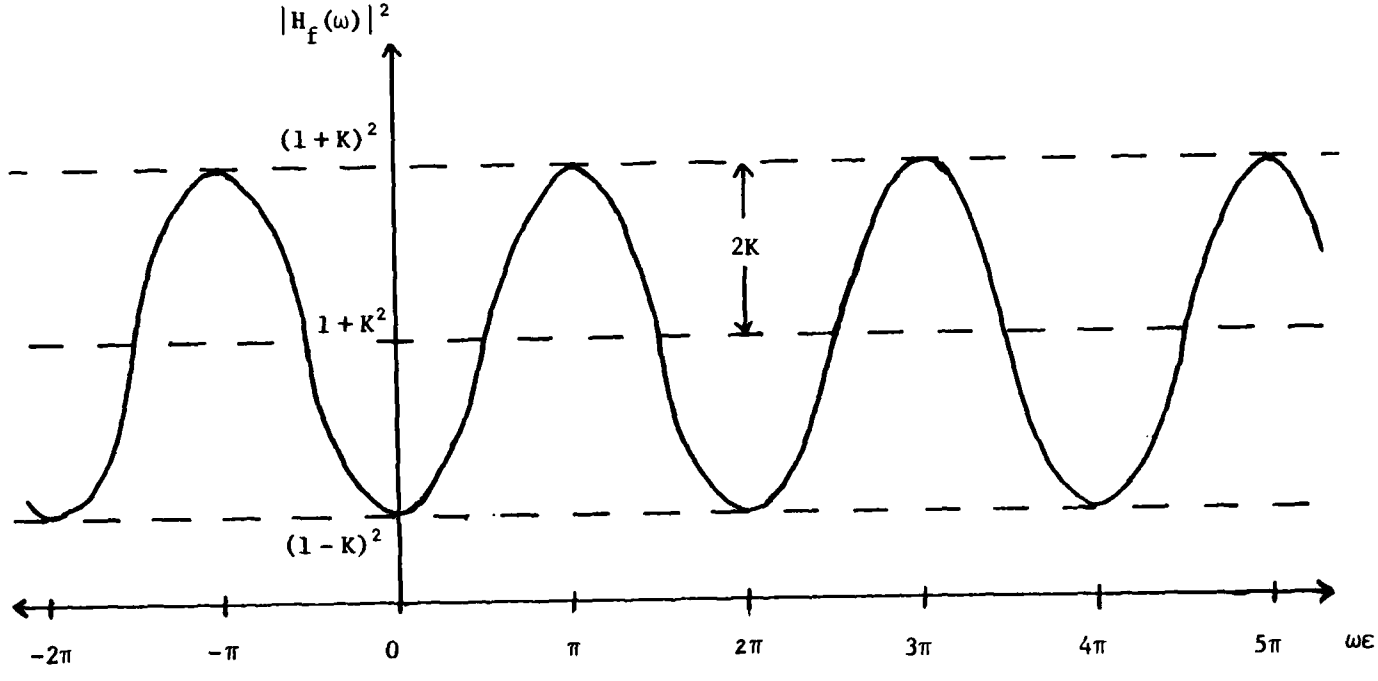

Fig. B-3 Square of magnitude of transfer function for feedforward control of wave propagation in structures versus parameter ($\omega\varepsilon$).

END

FILMED

3-86

DTIC